

Synthesis, Structure, and Reactions of Chiral Rhenium Vinylidene and Acetylide Complexes of the Formula $[(\eta^5\text{-C}_5\text{H}_5)\text{Re}(\text{NO})(\text{PPh}_3)(\text{X})]^{n+}$: Vinylidene Complexes That Are Formed by Stereospecific C_β Electrophilic Attack, Exist as Two $\text{Re}=\text{C}=\text{C}$ Geometric Isomers, and Undergo Stereospecific C_α Nucleophilic Attack

Dwayne R. Senn,^{1a} Andrew Wong,^{1b} Alan T. Patton,^{1a,b} Marianne Marsi,^{1b} Charles E. Strouse,^{1b} and J. A. Gladysz*,^{1a-c}

Contribution from the Departments of Chemistry, University of Utah, Salt Lake City, Utah 84112, and University of California, Los Angeles, California 90024. Received December 21, 1987

Abstract: Sequential reactions of acyl complexes $(\eta^5\text{-C}_5\text{H}_5)\text{Re}(\text{NO})(\text{PPh}_3)(\text{COCH}_2\text{R})$ (**2**: R = H (**a**), CH₃ (**b**), C₆H₅ (**c**), 1-naphthyl (**d**)) with $(\text{CF}_3\text{SO}_2)_2\text{O}$ (0.5 equiv), base (1.0 equiv), and $(\text{CF}_3\text{SO}_2)_2\text{O}$ (0.5 equiv) give vinylidene complexes $[(\eta^5\text{-C}_5\text{H}_5)\text{Re}(\text{NO})(\text{PPh}_3)(=\text{C}=\text{CHR})]^+\text{CF}_3\text{SO}_3^-$ (**3a-d** CF_3SO_3^- , 63–95%). Complexes **3b-d** CF_3SO_3^- crystallize as (95 ± 2):(5 ± 2), >99:1, and >99:1 mixtures of *sc/ac* $\text{Re}=\text{C}=\text{C}$ geometric isomers but equilibrate to (50 ± 2):(50 ± 2), (80 ± 2):(20 ± 2) and (80 ± 2):(20 ± 2) mixtures in CD_2Cl_2 . Photolysis gives (50 ± 2):(50 ± 2) photostationary states. An X-ray crystal structure of *sc-3d* PF_6^- ($\text{Re}=\text{C}_\alpha$ 1.840 (17) Å) shows a $\text{P}-\text{Re}-\text{C}_\beta-\text{C}_{\text{Np}}$ torsion angle of 161.5°, placing the naphthyl substituent anti to the bulky PPh_3 ligand. Reactions of **3a-d** CF_3SO_3^- with base give acetylide complexes $(\eta^5\text{-C}_5\text{H}_5)\text{Re}(\text{NO})(\text{PPh}_3)(\text{C}\equiv\text{CR})$ (**6a-d**, 59–93%). Reactions of **6b-d** with $\text{CF}_3\text{SO}_3\text{H}$ (–78 °C, assayed by NMR) give (98 ± 2):(2 ± 2), >99:1, and >99:1 mixtures of *ac-* and *sc-3b-d* CF_3SO_3^- . Analogous C_β methylation reactions (**6b-c**) are similarly stereospecific. This high 1,3-asymmetric induction is ascribed to electrophilic attack upon C_β of **6b-d** from a direction opposite to the PPh_3 ligand, giving the less stable $\text{Re}=\text{C}=\text{C}$ isomer with the C_β substituent syn to the PPh_3 ligand. Rates of *ac-3b-d* $\text{CF}_3\text{SO}_3^- \rightarrow$ *sc-3b-d* CF_3SO_3^- isomerization give $\Delta H^\ddagger = 20.8, 16.9, 18.6$ kcal/mol and $\Delta S^\ddagger = -5.7, -15.5, -10.5$ eu. A crystal structure of **6b** ($\text{Re}-\text{C}_\alpha$ 2.066 (7) Å) shows the $\text{ReC}\equiv\text{CCH}_3$ linkage to be essentially linear. Reactions of *ac-* and *sc-3b* CF_3SO_3^- with $\text{P}(\text{CH}_3)_3$ give (*Z*)- and (*E*)- $[(\eta^5\text{-C}_5\text{H}_5)\text{Re}(\text{NO})(\text{PPh}_3)(\text{C}(\text{P}(\text{CH}_3)_3)=\text{CHCH}_3)]^+\text{CF}_3\text{SO}_3^-$, respectively, indicating preferential attack upon the C_α face opposite to PPh_3 .

Transition-metal vinylidene complexes, $[\text{L}_n\text{M}=\text{C}=\text{CRR}']^{n+}$, have received extensive study over the last decade.²⁻¹² This interest

arises from a variety of factors. First, compounds that contain metal-carbon double bonds exhibit unique and diverse reactivity modes and structural properties. Second, surface-bound vinylidene ligands have been proposed to play a key role in hydrocarbon chain growth in the heterogeneously catalyzed Fischer-Tropsch process ("McCandlish mechanism").¹³ Third, vinylidene complexes have been shown to be effective acetylene polymerization catalyst precursors.^{10a} Fourth, vinylidene complexes show good potential for use in organic synthesis, such as in the preparation of β -lactams.¹⁴ Fifth, the parent vinylidene ligand, $=\text{C}=\text{CH}_2$, has been generated and spectroscopically characterized under high vacuum conditions on crystalline metal surfaces¹⁵ and under matrix

(1) (a) University of Utah. (b) University of California. (c) Address correspondence to this author at the University of Utah.

(2) Review: Bruce, M. I.; Swincer, A. G. *Adv. Organomet. Chem.* **1983**, 22, 59.

(3) (a) Davison, A.; Selegue, J. P. *J. Am. Chem. Soc.* **1978**, 100, 7763. (b) Adams, R. D.; Davison, A.; Selegue, J. P. *Ibid.* **1979**, 101, 7232. (c) Davison, A.; Selegue, J. P. *Ibid.* **1980**, 102, 2455.

(4) (a) Selegue, J. P. *J. Am. Chem. Soc.* **1982**, 104, 119. (b) Selegue, J. P. *Ibid.* **1983**, 105, 5921. (c) Iyer, R. S.; Selegue, J. P. *Ibid.* **1987**, 109, 910.

(5) (a) Boland, B. E.; Fam, S. A.; Hughes, R. P. *J. Organomet. Chem.* **1979**, 172, C29. (b) Boland-Lussier, B. E.; Churchill, M. R.; Hughes, R. P.; Rheingold, A. L. *Organometallics* **1982**, 1, 628. (c) Boland-Lussier, B. E.; Hughes, R. P. *Ibid.* **1982**, 1, 635.

(6) (a) Bruce, M. I. *Aust. J. Chem.* **1980**, 33, 1471. (b) Bruce, M. I.; Wong, F. S.; Skelton, B. W.; White, A. H. *J. Chem. Soc., Dalton Trans.* **1982**, 2203. (c) Bruce, M. I.; Humphrey, M. G.; Snow, M. R.; Tiekink, E. R. T. *J. Organomet. Chem.* **1986**, 314, 213. (d) Bruce, M. I.; Koutsantonis, G. A.; Liddell, M. J.; Nicholson, B. K. *Ibid.* **1987**, 320, 217. (e) Bruce, M. I.; Humphrey, M. G.; Liddell, M. J. *Ibid.* **1987**, 321, 91. (f) Bruce, M. I.; Humphrey, M. G.; Koutsantonis, G. A.; Liddell, M. J. *Ibid.* **1987**, 326, 247.

(7) (a) Davies, S. G.; Scott, F. J. *Organomet. Chem.* **1980**, 188, C41. (b) Abbott, S.; Davies, S. G.; Warner, P. *Ibid.* **1983**, 246, C65.

(8) (a) Wolf, J.; Werner, H.; Serhadli, O.; Ziegler, M. L. *Angew. Chem., Int. Ed. Engl.* **1983**, 22, 414. (b) Garcia Alonso, F. J.; Höhn, A.; Wolf, J.; Otto, H.; Werner, H. *Ibid.* **1985**, 24, 406. (c) Werner, H.; Garcia Alonso, F. J.; Otto, H.; Peters, K.; von Schnering, H. G. *J. Organomet. Chem.* **1985**, 289, C5. (d) Weinand, R.; Werner, H. *J. Chem. Soc., Chem. Commun.* **1985**, 1145. (e) Höhn, A.; Otto, H.; Dziallas, M.; Werner, H. *Ibid.* **1987**, 852. (f) Werner, H.; Wolf, J.; Garcia Alonso, F. J.; Ziegler, M. L.; Serhadli, O. *J. Organomet. Chem.* **1987**, 336, 397.

(9) (a) Consiglio, G.; Bangerter, F.; Darpin, C.; Morandini, F.; Lucchini, V. *Organometallics* **1984**, 3, 1446. (b) Consiglio, G.; Morandini, F.; Ciani, G. F.; Sironi, A. *Ibid.* **1986**, 5, 1976. (c) Consiglio, G.; Morandini, F. *Inorg. Chim. Acta* **1987**, 127, 79. (d) Consiglio, G.; Morandini, F. *Chem. Rev.* **1987**, 87, 761. (e) Consiglio, G.; Schwab, R.; Morandini, F. *J. Chem. Soc., Chem. Commun.* **1988**, 25.

(10) (a) Landon, S. J.; Shulman, P. M.; Geoffroy, G. L. *J. Am. Chem. Soc.* **1985**, 107, 6739. (b) Pourreau, D. B.; Geoffroy, G. L.; Rheingold, A. L.; Geib, S. J. *Organometallics* **1986**, 5, 1337.

(11) Structurally characterized rhenium vinylidene complexes: (a) Kolobova, N. E.; Antonova, A. B.; Khitrova, O. M.; Antipin, M. Yu.; Struchkov, Yu. T. *J. Organomet. Chem.* **1977**, 137, 69. (b) Pombeiro, A. J. L.; Jeffrey, J. C.; Pickett, C. J.; Richards, R. L. *Ibid.* **1984**, 277, C7.

(12) For other work on vinylidene complexes, see the following lead articles and references cited therein: (a) Antonova, A. B.; Kovalenko, S. V.; Korniyets, E. D.; Johansson, A. A.; Struchkov, Yu. T.; Ahmedov, A. I.; Yanovsky, A. I. *J. Organomet. Chem.* **1983**, 244, 35. (b) Roper, W. R.; Waters, J. M.; Wright, L. J.; van Meurs, F. *Ibid.* **1980**, 201, C27. (c) Berke, H.; Huttner, G.; von Seyler, J. *Ibid.* **1981**, 218, 193. (d) Beevor, R. G.; Freeman, M. J.; Green, M.; Morton, C. E.; Orpen, A. G. *J. Chem. Soc., Chem. Commun.* **1985**, 68. (e) Chan, Y. W.; Renner, M. W.; Balch, A. L. *Organometallics* **1983**, 2, 1888. (f) Reger, D. L.; Swift, C. A. *Ibid.* **1984**, 3, 876. (g) Mayr, A.; Schaefer, K. C.; Huang, E. Y. *J. Am. Chem. Soc.* **1984**, 106, 1517. (h) Birdwhistell, K. R.; Tonker, T. L.; Templeton, J. L. *Ibid.* **1985**, 107, 4474. (i) Collman, J. P.; Brothers, P. J.; McElwee-White, L.; Rose, E. *Ibid.* **1985**, 107, 6110. (j) van Asselt, A.; Burger, B. J.; Gibson, V. C.; Bercaw, J. E. *Ibid.* **1986**, 108, 5347. (k) Bullock, R. M. *Ibid.* **1987**, 109, 8087.

(13) (a) McCandlish, L. E. *J. Catal.* **1983**, 83, 362. (b) Hoel, E. L.; Ansell, G. B.; Leta, S. *Organometallics* **1986**, 5, 585. (c) Hoel, E. L. *Ibid.* **1986**, 5, 587.

(14) (a) Barrett, A. G. M.; Sturgess, M. A. *Tetrahedron Lett.* **1986**, 27, 3811; *J. Org. Chem.* **1987**, 52, 3940. (b) Liebeskind, L. S.; Chidambaram, R. *J. Am. Chem. Soc.* **1987**, 109, 5025. (c) Barrett, A. G. M.; Carpenter, N. E. *Organometallics* **1987**, 6, 2249.

(15) Hills, M. M.; Parmeter, J. E.; Weinberg, W. H. *J. Am. Chem. Soc.* **1987**, 109, 597.

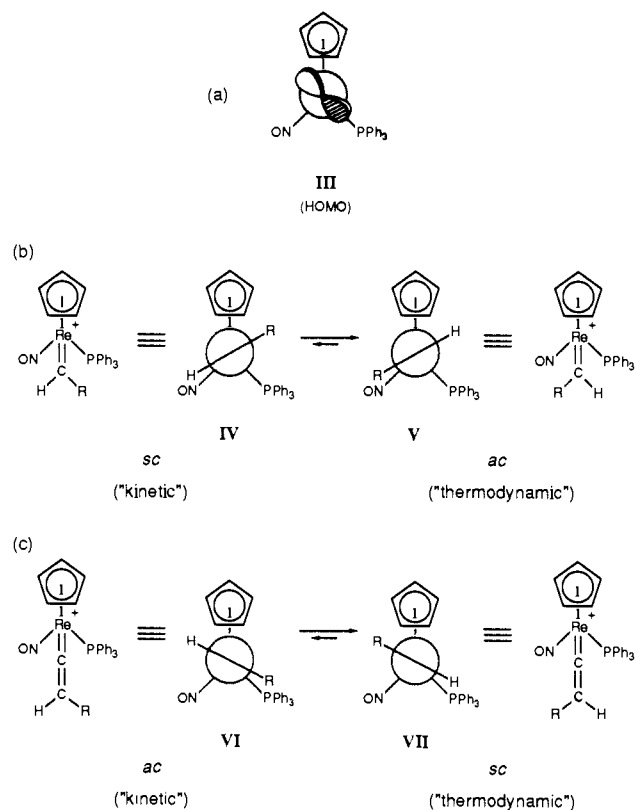
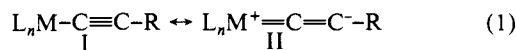


Figure 1. Comparison of (a) the HOMO of the $(\eta^5\text{-C}_5\text{H}_5)\text{Re}(\text{NO})(\text{PPh}_3)^+$ fragment with (b) $\text{Re}=\text{C}_\alpha$ geometric isomers in alkylidene complexes $[(\eta^5\text{-C}_5\text{H}_5)\text{Re}(\text{NO})(\text{PPh}_3)(=\text{CHR})]^+$ and (c) $\text{Re}=\text{C}=\text{C}_\beta$ geometric isomers in vinylidene complexes $[(\eta^5\text{-C}_5\text{H}_5)\text{Re}(\text{NO})(\text{PPh}_3)(=\text{C}=\text{CHR})]^+$.

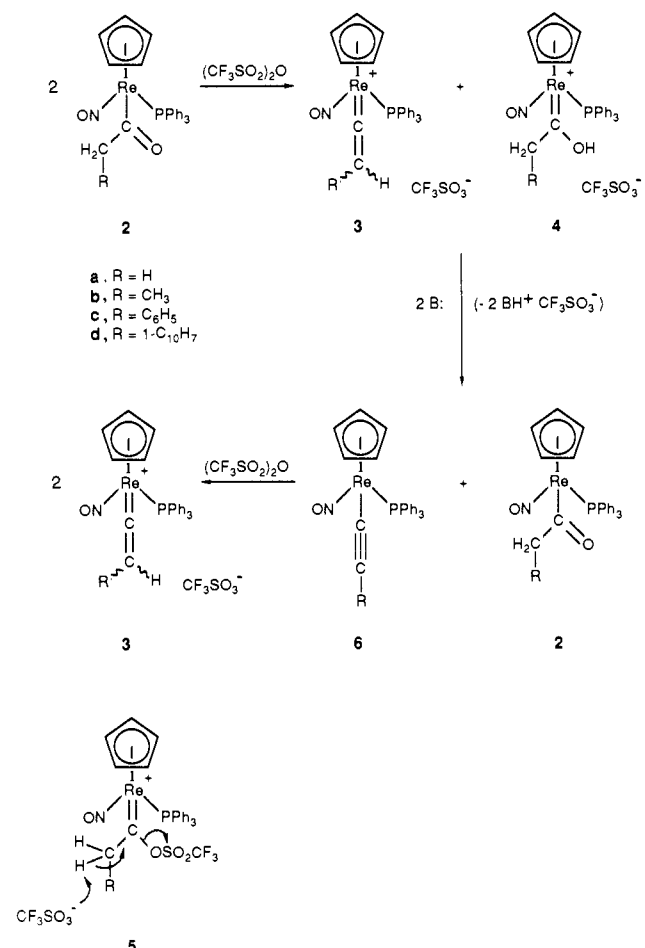
isolation conditions on single metal centers.¹⁶ Finally, free vinylidene $\text{C}=\text{CH}_2$ rapidly rearranges to acetylene ($<10^{-12}$ s) and thus, unlike metal vinylidene complexes, is not readily amenable to direct study.¹⁷

Transition-metal acetylide or alkynyl complexes, $\text{L}_n\text{MC}\equiv\text{CR}$, are common precursors to, and reaction products of, vinylidene complexes.^{18,19} Their structural features and reactivity are also of fundamental interest, and they provide an opportunity to define transition-metal substituent effects upon $\text{C}\equiv\text{C}$ triple bond properties.²⁰ Acetylide complexes of electron-donating L_nM -systems should have two important resonance contributors, I and II, as shown in eq 1. Such acetylide complexes should, like yneamines $(\text{R}_2\text{N}\text{C}\equiv\text{CR})$,²¹ be nucleophilic at C_β .



We have previously shown that the chiral rhenium fragment $(\eta^5\text{-C}_5\text{H}_5)\text{Re}(\text{NO})(\text{PPh}_3)^+$ is a powerful π donor, with the high-lying d orbital HOMO shown in Figure 1a.²² We have also

Scheme I. Synthesis of Vinylidene Complexes $[(\eta^5\text{-C}_5\text{H}_5)\text{Re}(\text{NO})(\text{PPh}_3)(=\text{C}=\text{CHR})]^+\text{CF}_3\text{SO}_3^-$ ($3\text{CF}_3\text{SO}_3^-$)



reported that the corresponding rhenium alkylidene complexes $[(\eta^5\text{-C}_5\text{H}_5)\text{Re}(\text{NO})(\text{PPh}_3)(=\text{CHR})]^+\text{PF}_6^-$ can easily be prepared as either of the two $\text{Re}=\text{C}$ geometric isomers illustrated in Figure 1b as well as in optically pure form.^{22,23} Overlap of the rhenium fragment HOMO with the $=\text{CHR}$ ligand p acceptor orbital is maximized in each isomer. These complexes undergo stereospecific or stereoselective C_α nucleophilic (Nu^-) attack to give alkyl complexes of the formula $(\eta^5\text{-C}_5\text{H}_5)\text{Re}(\text{NO})(\text{PPh}_3)(\text{CHRNu})$ in high diastereomeric excess. We have also shown that chiral rhenium vinyl complexes $(\eta^5\text{-C}_5\text{H}_5)\text{Re}(\text{NO})(\text{PPh}_3)(\text{CX}=\text{CRR}')$ undergo stereoselective C_β electrophilic (E^+) attack to give alkylidene complexes of the formula $[(\eta^5\text{-C}_5\text{H}_5)\text{Re}(\text{NO})(\text{PPh}_3)(=\text{CXCRR}'\text{E})]^+$ in high diastereomeric excess.²⁴ Hence, we sought to determine whether similar structural and chemical phenomena would be exhibited by analogous rhenium vinylidene and acetylide complexes.

In this paper, we report (a) high-yield syntheses of chiral rhenium vinylidene complexes $[(\eta^5\text{-C}_5\text{H}_5)\text{Re}(\text{NO})(\text{PPh}_3)(=\text{C}=\text{CRR}')^+\text{X}^-$ and acetylide complexes $(\eta^5\text{-C}_5\text{H}_5)\text{Re}(\text{NO})(\text{PPh}_3)(\text{C}\equiv\text{CR})$, (b) the first observation of $\text{M}=\text{C}=\text{C}$ geometric isomerism in vinylidene complexes, (c) the thermal and photochemical interconversion of these geometric isomers and the

(16) Kline, E. S.; Kafafi, Z. H.; Hauge, R. H.; Margrave, J. L. *J. Am. Chem. Soc.* **1987**, *109*, 2402.

(17) Durán, R. P.; Amorebieta, V. T.; Colussi, A. J. *J. Am. Chem. Soc.* **1987**, *109*, 3154.

(18) Review: Nast, R. *Coord. Chem. Rev.* **1982**, *47*, 89.

(19) Many of the articles cited in ref 2-12 also deal with acetylide complexes. See also the following references: (a) Bruce, M. I.; Harbourne, D. A.; Waugh, F.; Stone, F. G. A. *J. Chem. Soc. A* **1968**, 356. (b) Sieber, W.; Wolfgruber, M.; Neugebauer, D.; Orama, O.; Kreißl, F. R. *Z. Naturforsch. B: Anorg. Chem., Org. Chem.* **1983**, *38b*, 67. (c) Consiglio, G.; Morandini, F.; Sironi, A. *J. Organomet. Chem.* **1986**, *306*, C45. (d) Buang, N. A.; Hughes, D. L.; Kashef, N.; Richards, R. L.; Pombeiro, A. J. L. *Ibid.* **1987**, *323*, C47. (e) Marder, T. B.; Zargarian, D.; Calabrese, J. C.; Herskovitz, T. H.; Milstein, D. *J. Chem. Soc., Chem. Commun.* **1987**, 1484.

(20) Kostič, N. M.; Fenske, R. F. *Organometallics* **1982**, *1*, 974.

(21) (a) Ficini, J. *Tetrahedron* **1976**, *32*, 1449. (b) Pitacco, G.; Valentin, E. In *The Chemistry of Amino, Nitroso and Nitro Compounds and Their Derivatives; Supplement F, Part 1*; Patai, S., Ed.; Wiley: New York, 1985; Chapter 15.

(22) (a) Kiel, W. A.; Lin, G.-Y.; Constable, A. G.; McCormick, F. B.; Strouse, C. E.; Eisenstein, O.; Gladysz, J. A. *J. Am. Chem. Soc.* **1982**, *104*, 4865. (b) Kiel, W. A.; Lin, G.-Y.; Bodner, G. S.; Gladysz, J. A. *Ibid.* **1983**, *105*, 4958. (c) Kiel, W. A.; Buhro, W. E.; Gladysz, J. A. *Organometallics* **1984**, *3*, 879. (d) Georgiou, S.; Gladysz, J. A. *Tetrahedron* **1986**, *42*, 1109. (e) O'Connor, E. J.; Kobayashi, M.; Floss, H. G.; Gladysz, J. A. *J. Am. Chem. Soc.* **1987**, *109*, 4837.

(23) Merrifield, J. H.; Strouse, C. E.; Gladysz, J. A. *Organometallics* **1982**, *1*, 1204.

(24) Bodner, G. S.; Smith, D. E.; Hatton, W. G.; Heah, P. C.; Georgiou, S.; Rheingold, A. L.; Geib, S. J.; Hutchinson, J. P.; Gladysz, J. A. *J. Am. Chem. Soc.* **1987**, *109*, 7688.

corresponding rates and activation parameters, (d) examples of stereospecific C_α nucleophilic attack upon the vinylidene complexes and stereospecific C_β electrophilic attack upon the acetylide complexes, and (e) X-ray crystal structures that establish the stereochemistry of these transformations and bonding features of both types of complexes. A portion of this study has been communicated.²⁵

Results

1. Syntheses of Vinylidene Complexes $[(\eta^5\text{-C}_5\text{H}_5)\text{Re}(\text{NO})(\text{PPh}_3)(=\text{C}=\text{CHR})]^+\text{CF}_3\text{SO}_3^-$. The "methyl ester" $(\eta^5\text{-C}_5\text{H}_5)\text{Re}(\text{NO})(\text{PPh}_3)(\text{CO}_2\text{CH}_3)$ (**1**) was treated with Grignard reagents RCH_2MgBr as previously reported²⁶ to give the known acyl complexes $(\eta^5\text{-C}_5\text{H}_5)\text{Re}(\text{NO})(\text{PPh}_3)(\text{COCH}_2\text{R})$ (**2**; **a**, $\text{R} = \text{H}$; **b**, $\text{R} = \text{CH}_3$; **c**, $\text{R} = \text{C}_6\text{H}_5$). Reaction of **1** and the Grignard reagent derived from 1-(chloromethyl)naphthalene, $1\text{-C}_{10}\text{H}_7\text{CH}_2\text{MgCl}$, gave the new acyl complex $(\eta^5\text{-C}_5\text{H}_5)\text{Re}(\text{NO})(\text{PPh}_3)(\text{COCH}_2(1\text{-C}_{10}\text{H}_7))$ (**2d**, 76%).

Acyl complexes **2a-d** were treated with 1.0 equiv of triflic anhydride, $(\text{CF}_3\text{SO}_2)_2\text{O}$ (Scheme I). This reagent had previously been shown by Hughes to efficiently convert iron acyl complexes $(\eta^5\text{-C}_5\text{H}_5)\text{Fe}(\text{CO})(\text{PPh}_3)(\text{COCH}_2\text{R})$ to observable carbene complexes $[(\eta^5\text{-C}_5\text{H}_5)\text{Fe}(\text{CO})(\text{PPh}_3)(=\text{C}(\text{OSO}_2\text{CF}_3)\text{CH}_2\text{R})]^+\text{CF}_3\text{SO}_3^-$, which then fragmented to the corresponding vinylidene complexes $[(\eta^5\text{-C}_5\text{H}_5)\text{Re}(\text{NO})(\text{PPh}_3)(=\text{C}=\text{CHR})]^+\text{CF}_3\text{SO}_3^-$ (**3a-dCF}_3\text{SO}_3^-)²⁷ and undesired hydroxycarbene complexes $[(\eta^5\text{-C}_5\text{H}_5)\text{Re}(\text{NO})(\text{PPh}_3)(=\text{C}(\text{OH})\text{CH}_2\text{R})]^+\text{CF}_3\text{SO}_3^-$ (**4a-dCF}_3\text{SO}_3^-). Identical mixtures were obtained with 0.5 equiv or large excesses of $(\text{CF}_3\text{SO}_2)_2\text{O}$. Hydroxycarbene complexes **4a-bCF}_3\text{SO}_3^- have previously been shown to rapidly form from acyl complexes **2a-b** and $\text{CF}_3\text{SO}_3\text{H}$.²⁶ Hence, the probable initial intermediate in Scheme I, carbene complex $[(\eta^5\text{-C}_5\text{H}_5)\text{Re}(\text{NO})(\text{PPh}_3)(=\text{C}(\text{OSO}_2\text{CF}_3)\text{CH}_2\text{R})]^+\text{CF}_3\text{SO}_3^-$ (**5**, Scheme I), likely fragments to $\text{CF}_3\text{SO}_3\text{H}$ and $3\text{CF}_3\text{SO}_3^-$ at a rate faster than its formation.******

This problem was circumvented by treating the $3\text{CF}_3\text{SO}_3^-/4\text{CF}_3\text{SO}_3^-$ mixtures with 1 equiv of the bases $\text{K}^+t\text{-BuO}^-$ or TMP .^{27d} Both cationic compounds were deprotonated (Scheme I) to give 50:50 mixtures of acetylide complexes $(\eta^5\text{-C}_5\text{H}_5)\text{Re}(\text{NO})(\text{PPh}_3)(\text{C}\equiv\text{CR})$ (**6**; isolated below) and acyl complexes **2**. These mixtures were then treated with 0.5 equiv of $(\text{CF}_3\text{SO}_2)_2\text{O}$. The remaining acyl complex **2** was converted to $3\text{CF}_3\text{SO}_3^-$, and the acetylide complex **6** acted as a base for the $\text{CF}_3\text{SO}_3\text{H}$ liberated. This multistep but convergent "one-pot" preparation gave vinylidene complexes **3a-dCF}_3\text{SO}_3^- as crude powders in 84–95% yields.**

2. Characterization of Vinylidene Complexes. Subsequent crystallization gave analytically pure **3b-dCF}_3\text{SO}_3^- (63–78% from **2b-d**), which were characterized by IR and ^1H , $^{13}\text{C}\{^1\text{H}\}$, and $^{31}\text{P}\{^1\text{H}\}$ NMR spectroscopy (Table I). The crystals were dissolved in CD_2Cl_2 at -78°C , and ^1H NMR spectra were immediately recorded at -80°C . It was thus shown that crystalline **3b-dCF}_3\text{SO}_3^- consisted of $(95 \pm 2):(5 \pm 2)$, $>99:1$, and $>99:1$ mixtures of *sc/ac*^{27a} $\text{Re}=\text{C}=\text{C}$ geometric isomers (Figure 1), respectively. The solutions were kept at room temperature for 24 h, after which time $(50 \pm 2):(50 \pm 2)$, $(80 \pm 2):(20 \pm 2)$, and $(80 \pm 2):(20 \pm 2)$ *sc/ac* equilibrium mixtures were present (see Scheme II). The geometric isomer assignments were made in anticipation that the vinylidene ligand would prefer to adopt****

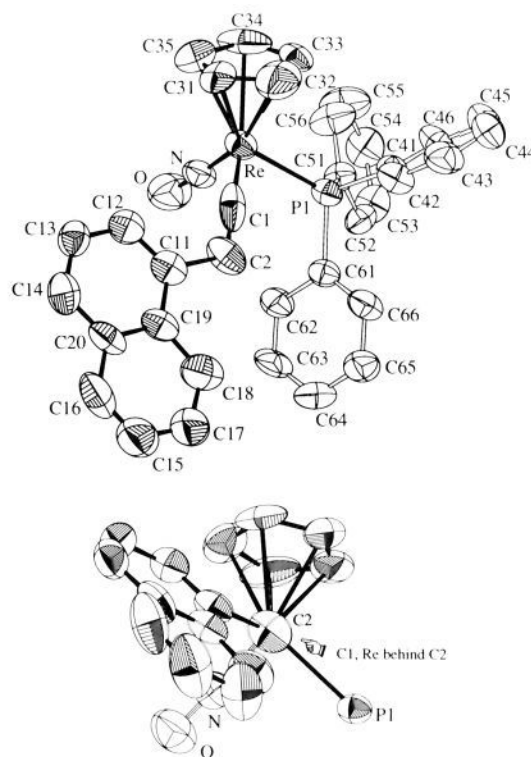


Figure 2. Structure of the cation of naphthylvinylidene complex $sc\text{-}[(\eta^5\text{-C}_5\text{H}_5)\text{Re}(\text{NO})(\text{PPh}_3)(=\text{C}=\text{CH}(1\text{-C}_{10}\text{H}_7))]^+\text{PF}_6^-$ (*sc*-**3dPF}_6^-**). Top: numbering diagram; bottom: Newman projection down $\text{C}_2\text{-C}_1\text{-Re}$ with phenyl rings omitted.

conformations VI (*ac*) and VII (*sc*; Figure 1c), which maximize overlap of the rhenium fragment d orbital HOMO (see III) with the C_α p acceptor orbital, and that steric interaction between the bulky PPh_3 ligand and the C_β alkyl substituent would destabilize VI. These assumptions were verified as described below.

Vinylidene complexes **3a-dCF}_3\text{SO}_3^- exhibited several noteworthy spectroscopic features. The $\eta^5\text{-C}_5\text{H}_5$ ligand ^1H NMR resonances (ca. δ 6.00) were among the furthest downfield observed in cationic rhenium complexes $[(\eta^5\text{-C}_5\text{H}_5)\text{Re}(\text{NO})(\text{PPh}_3)(\text{X})]^+$, in accord with the high π acidity of vinylidene ligands.²⁰ The IR $\nu_{\text{N}=\text{O}}$ were also greater than usual, and weak $\nu_{\text{C}=\text{C}}$ were present. Downfield C_α resonances were noted in ^{13}C NMR spectra. Solutions of **3a-dCF}_3\text{SO}_3^- were yellow to yellow-brown, and naphthylvinylidene complex **3dCF}_3\text{SO}_3^- exhibited a long wavelength UV absorption at 367 nm (ϵ 7600; Experimental Section). This band was absent in **3bCF}_3\text{SO}_3^- and naphthalene.********

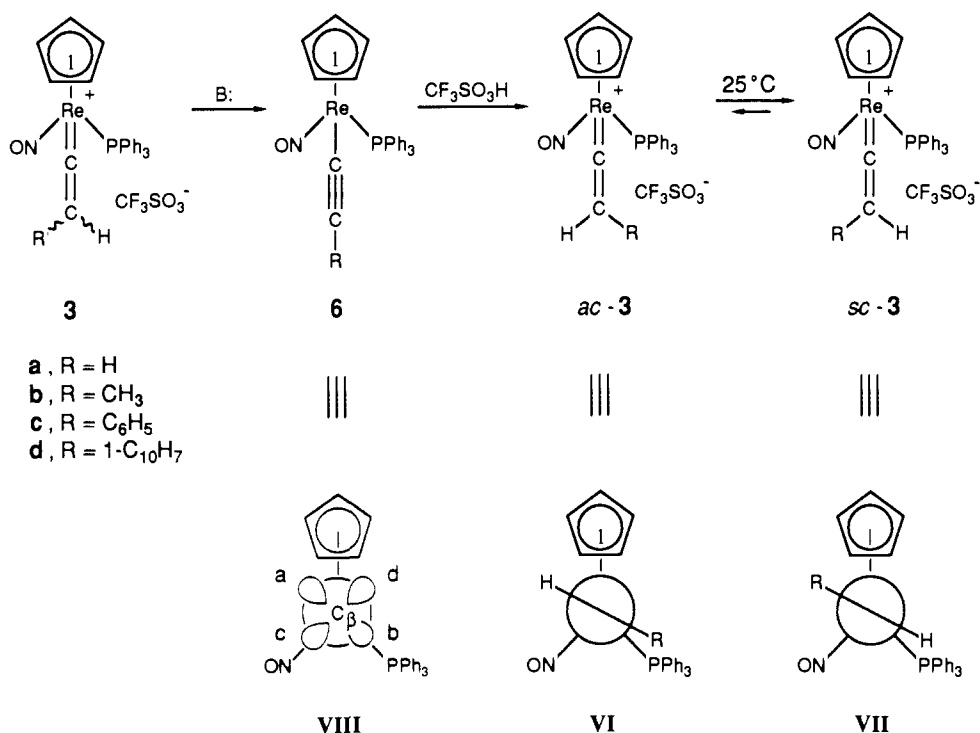
Assignments of NMR resonances to *sc/ac* isomers were made on the basis of the enriched samples described above and the stereospecific syntheses given below. The C_β protons in the *sc* isomers VII, which are syn to the PPh_3 ligand, were upfield of those in the *ac* isomers VI. Hence, the upfield $=\text{CH}_2$ resonance of parent vinylidene complex **3aCF}_3\text{SO}_3^- was assigned to the proton syn to PPh_3 (H_{sc} ^{27a}). Finally, the PPh_3 ^{13}C NMR resonances of naphthylvinylidene complex *ac*-**3dCF}_3\text{SO}_3^-, which has the naphthyl group directed toward the PPh_3 ligand, were poorly resolved at -80 to -50°C . However, sharp resonances were observed for the more stable $\text{Re}=\text{C}=\text{C}$ isomer, *sc*-**3dCF}_3\text{SO}_3^- (-80°C). This suggests increased rotational barriers for the Re-P and/or P-C bonds in *ac*-**3dCF}_3\text{SO}_3^-.********

3. X-ray Crystal Structure of *sc*- $(\eta^5\text{-C}_5\text{H}_5)\text{Re}(\text{NO})(\text{PPh}_3)(=\text{C}=\text{CH}(1\text{-C}_{10}\text{H}_7))^+\text{PF}_6^-$ (*sc*-3dPF}_6^-**).** Difficulty was encountered in obtaining vinylidene complex crystals suitable for X-ray analysis or in solving the subsequent data sets. Finally, crystals of naphthylvinylidene complex *sc*-**3dPF}_6^- were obtained as described below. X-ray data were acquired as summarized in Table II. Refinement, described in the Experimental Section, yielded the structure shown in Figure 2. Positional parameters, bond distances, and bond angles are summarized in Tables III–V.**

(25) Wong, A.; Gladysz, J. A. *J. Am. Chem. Soc.* **1982**, *104*, 4948.

(26) Buhro, W. E.; Wong, A.; Merrifield, J. H.; Lin, G.-Y.; Constable, A. G.; Gladysz, J. A. *Organometallics* **1983**, *2*, 1852.

(27) Nomenclature conventions: (a) In synclinal (*sc*) $\text{Re}=\text{C}=\text{C}$ isomers, the highest priority^{27b} ligands on Re ($\eta^5\text{-C}_5\text{H}_5$) and C_β define a $60 \pm 30^\circ$ torsion angle; in anticlinal (*ac*) isomers, the highest priority ligands define a $120 \pm 30^\circ$ torsion angle. *Pure Appl. Chem.* **1976**, *45*, 11; see section E-5.6, p 24. (b) The $\eta^5\text{-C}_5\text{H}_5$ ligand is considered to be a pseudoatom of atomic number 30, which gives the following priority sequence: $\eta^5\text{-C}_5\text{H}_5 > \text{PPh}_3 > \text{NO} > \text{C}=\text{CHR}$. (c) Compounds not indicated to be specific $\text{Re}=\text{C}=\text{C}$ isomers are mixtures of isomers. (d) $\text{TMP} = 2,2,6,6\text{-tetramethylpiperidine}$. (e) $\text{dppe} = \text{Ph}_2\text{PCH}_2\text{CH}_2\text{PPh}_2$.

Scheme II. Interconversion of Vinylidene Complexes $3\text{CF}_3\text{SO}_3^-$ and Acetylide Complexes $(\eta^5\text{-C}_5\text{H}_5)\text{Re}(\text{NO})(\text{PPh}_3)(\text{C}\equiv\text{CR})$ (**6**)Kinetic ratios (*ac/sc*)

3b	(98 ± 2):(2 ± 2)
3c	>99:1
3d	>99:1

Equilibrium ratios (*ac/sc*)

3b	(50 ± 2):(50 ± 2)
3c	(20 ± 2):(80 ± 2)
3d	(20 ± 2):(80 ± 2)

The Newman projection in the bottom part of Figure 2 illustrates the anti relationship of the C_β naphthyl substituent and the PPh₃ ligand in *sc-3d*PF₆⁻ (compare VII), thus confirming the Re=C=C geometric isomer assignments made above. The C_β-C_{Np} (C2-C11) bond defines 161.5° and 71.0° torsion angles with the Re-P1 and Re-N bonds, respectively. Although the C_β hydrogen was not located, its calculated position extends over the π cloud of the C61-C66 PPh₃ phenyl ring. Distances to the phenyl carbons range from 3.24-3.29 Å (C61, C66) to 3.84-3.91 Å (C63, C64). This accounts for the upfield ¹H NMR shifts in *sc* Re=C=C isomers noted above.

4. Syntheses and Characterization of Acetylide Complexes $(\eta^5\text{-C}_5\text{H}_5)\text{Re}(\text{NO})(\text{PPh}_3)(\text{C}\equiv\text{CR})$ (6**).** Vinylidene complexes **3a-d**CF₃SO₃⁻ were treated with bases K⁺-*t*-BuO⁻ or TMP.^{27d} Workup gave acetylide complexes **6a-d** as powders in 53-93% yields (Scheme II). Subsequent crystallization gave analytically pure **6b-d** (72-82% from **3d-d**CF₃SO₃⁻).

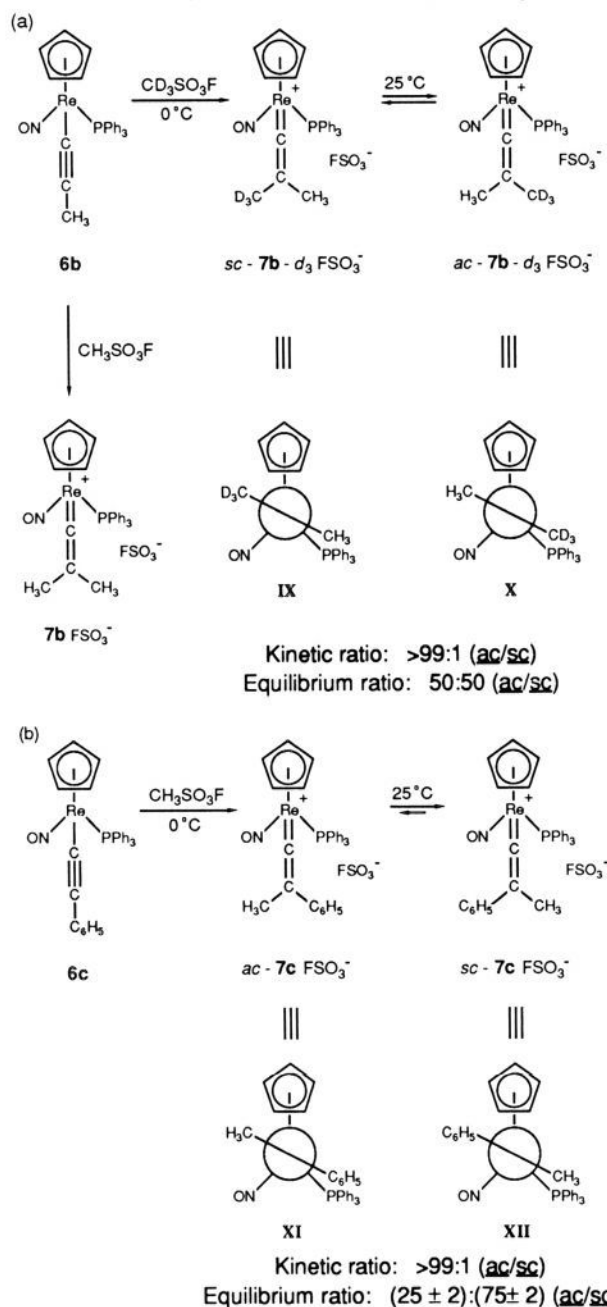
Acetylide complexes **6a-d** were characterized by IR and ¹H, ¹³C{¹H}, and ³¹P{¹H} NMR spectroscopy (Table VI). In all cases, diagnostic weak IR ν_{C=C} were observed. The parent acetylide complex **6a** exhibited a sharp, medium IR ν_{C-H} at 3282 cm⁻¹. This assignment was confirmed by the observation of an IR ν_{C-D} at 2268 cm⁻¹ in deuterioacetylide complex **6a-d.²⁸ A proton-coupled ¹³C NMR spectrum of **6a** showed C_β (¹J_{CH} = 228 Hz) to be downfield of C_α (²J_{CH} = 39.4 Hz). The C_α carbon also showed an appreciable ²J_{CP}, whereas ³J_{CP} for C_β was <1 Hz. The downfield C≡C resonances of **6b-d** also showed ³J_{CP} of <1 Hz and were accordingly assigned to C_β. Solutions of **6a-d** were**

orange-red, and naphthyl acetylide complex **6d** showed pronounced longer wavelength UV absorptions (Experimental Section) at 320 nm (ε 16 000) and 360 nm (sh, ε 7900). These bands were absent in **6b** and naphthalene.

5. Reactions of Acetylide Complexes with Electrophiles. 1,3-Asymmetric Induction. Reaction of methyl acetylide complex **6b** and CF₃SO₃H (1.0 equiv, CD₂Cl₂) was monitored by ¹H NMR at -78 °C. Methylvinylidene complex **3b**CF₃SO₃⁻ rapidly formed as a (98 ± 2):(2 ± 2) mixture of *ac/sc* isomers (Scheme II). Aryl acetylide complexes **6c-d** were similarly treated with CF₃SO₃H. This gave arylvinylidene complexes *ac-3c-d*CF₃SO₃⁻ as >99:1 mixtures of *ac/sc* isomers. As a check, these solutions were kept at 25 °C for 24 h, and the equilibrium *sc/ac* isomer ratios noted above were obtained. These data are consistent with a transition state in which the protic electrophile approaches C_β from a direction opposite to the bulky PPh₃ ligand. Such a transition state would give the *less* stable Re=C=C isomer when the electrophile is smaller than the acetylide complex C_β substituent. Reaction of **6d** with HPF₆·Et₂O and room temperature workup gave the sample of *sc-3d*PF₆⁻ used in the above crystal structure.

The reaction of methyl acetylide complex **6b** and methylating agent CH₃SO₃F (CD₂Cl₂, -78 °C) was monitored by ¹H NMR. Dimethylvinylidene complex [(η⁵-C₅H₅)Re(NO)(PPh₃)(=C=C(CH₃)₂)]⁺F₃SO₃⁻ (**7b**F₃SO₃⁻) formed cleanly at 0 °C (Scheme IIIa) and was isolated in 80% yield after recrystallization. Two ¹H NMR methyl resonances were observed (δ 1.96, 1.24; Table I). Similar reaction of **6b** with the deuterated methylating agent CD₃SO₃F gave *sc*-[(η⁵-C₅H₅)Re(NO)(PPh₃)(=C=C(CH₃)₂)]⁺F₃SO₃⁻ (*sc-7b-d*₃F₃SO₃⁻; IX), in which the downfield δ 1.96 resonance of **7b**F₃SO₃⁻ was absent (detection limit 1%). Upon warming the sample above 0 °C, the δ 1.96 resonance appeared

(28) Complex **6a-d₁ was prepared from deuterioacetyl complex **2a-d₃, which was in turn synthesized from **1** and CD₃MgI.²⁶****

Scheme III. Stereospecific Methylation of Acetylide Complexes **6**

as the δ 1.24 resonance diminished. After 18 h at 25 °C, both resonances were of equal intensity. Thus, methylation of **6b** occurred stereospecifically, and the stereochemistry was assigned (Scheme IIIa) by analogy to the above protonation reactions. Accordingly, the upfield methyl ^1H NMR resonance of **7b** FSO_3^- (δ 1.24) was assigned to the methyl group syn to the PPh_3 ligand (*ac*- CH_3 ^{27a}), consistent with the C_β proton shielding trends noted above.

The reaction of phenyl acetylide complex **6c** and $\text{CH}_3\text{SO}_3\text{F}$ was similarly monitored by ^1H NMR (Scheme IIIb). At 0 °C, methyl phenyl vinylidene complex *ac*-[(η^5 - C_5H_5) $\text{Re}(\text{NO})(\text{PPh}_3)(=\text{C}=\text{C}(\text{CH}_3)(\text{C}_6\text{H}_5))^+\text{FSO}_3^-$] (*ac*-**7c** FSO_3^- ; **XI**) formed as a single $\text{Re}=\text{C}=\text{C}$ isomer, the stereochemistry of which was assigned by analogy to the above reactions. Complex *ac*-**7c** FSO_3^- equilibrated to a (75 ± 2):(25 ± 2) *sc/ac* mixture over the course of 4 h at 30–45 °C. Hence, as with the protonation of **6c**, the less stable $\text{Re}=\text{C}=\text{C}$ isomer formed initially. As expected, the ^1H NMR methyl resonance of the *sc* isomer (**XII**; δ 1.58) was upfield of that of the *ac* isomer (**XI**; δ 2.33).

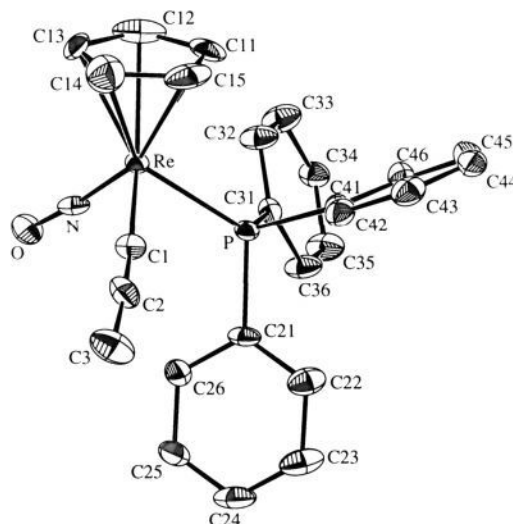
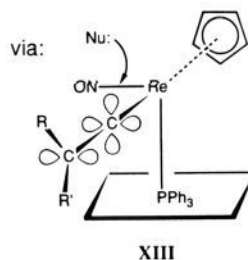
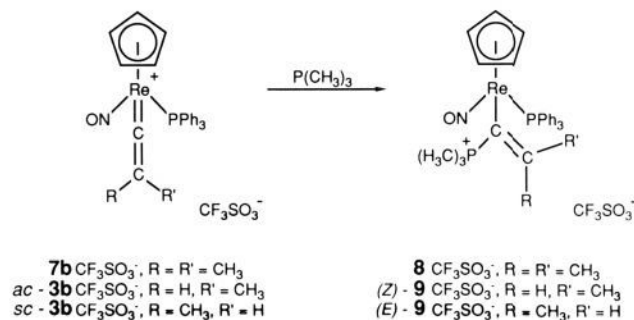


Figure 3. Molecular structure of methyl acetylide complex (η^5 - C_5H_5) $\text{Re}(\text{NO})(\text{PPh}_3)(\text{C}\equiv\text{CCH}_3)$ (**6b**).

Scheme IV. Reactions of Vinylidene Complexes with $\text{P}(\text{CH}_3)_3$: Stereochemistry of C_α Attack

6. X-ray Crystal Structure of Methyl Acetylide Complex (η^5 - C_5H_5) $\text{Re}(\text{NO})(\text{PPh}_3)(\text{C}\equiv\text{CCH}_3)$ (6b**).** We sought to determine whether a distortion of the ideally linear $\text{Re}-\text{C}_\alpha=\text{C}_\beta-\text{R}$ linkage in acetylide complexes **6a–d** might contribute to the stereospecificity of C_β electrophilic attack. Hence, X-ray data were collected for methyl acetylide complex **6b** as summarized in Table II. Refinement, described in the Experimental Section, yielded the structure shown in Figure 3. The near-linearity of the $\text{Re}-\text{C}_\alpha=\text{C}_\beta$ ($\text{Re}-\text{C}1-\text{C}2$) and $\text{C}_\alpha=\text{C}_\beta-\text{C}_\gamma$ ($\text{C}1-\text{C}2-\text{C}3$) linkages (176–177°) is evident. Positional parameters, bond distances, and bond angles are summarized in Tables VII–IX.

7. Rates of Interconversion of Vinylidene Complex $\text{Re}=\text{C}=\text{C}$ Isomers. The rates of $\text{Re}=\text{C}=\text{C}$ isomerization of vinylidene complexes *ac*-**3b–d** CF_3SO_3^- were measured as outlined in Table X. The *ac* \rightleftharpoons *sc* K_{eq} , which were needed to extract k_1 from k_{obsd} , did not change significantly over the temperature range of the rate measurements. The k_1 values gave the activation parameters summarized in Table X.

Control experiments were conducted to probe whether $\text{Re}=\text{C}=\text{C}$ isomerization might occur by a C_β deprotonation/protonation mechanism. First, similar isomerization rates and acti-

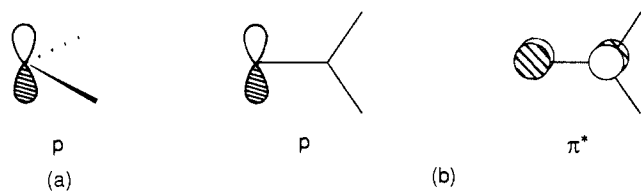


Figure 4. Comparison of vacant acceptor orbitals in (a) alkylidene and (b) vinylidene ligands.

vation parameters were obtained for methyl phenyl vinylidene complex *ac*-**7c**FSO₃⁻ (Table X), which lacks a C_β proton. Second, the concentration of the CF₃SO₃⁻ counteranion, the most plausible proton carrier, was varied. The isomerization rate of *ac*-**3d**CF₃SO₃⁻ was measured in the presence of added (*n*-C₄H₉)₄N⁺CF₃SO₃⁻ (0.27 equiv). This gave *k*₁ = 6.20 × 10⁻⁴ s⁻¹ (25.4 °C), slightly lower than that without added triflate (6.75 × 10⁻⁴ s⁻¹, 24.6 °C). Tetrafluoroborate complexes *ac*-**3c**BF₄⁻ and *ac*-**3d**BF₄⁻ were generated from HBF₄·Et₂O and the corresponding acetylide complexes at -78 °C. Their isomerization rates (*k*₁ = 6.27 × 10⁻⁴ s⁻¹ (22.2 °C) and 5.27 × 10⁻⁴ s⁻¹ (25.4 °C)) were comparable to those in Table X. Hence, it is concluded that Re=C=C isomerization occurs predominantly or exclusively by simple bond rotation.

The ¹H NMR spectra of parent vinylidene complex **3a**CF₃SO₃⁻, methylvinylidene complex **3b**CF₃SO₃⁻, and dimethylvinylidene complex **7b**FSO₃⁻ were recorded at 110 °C and 200 MHz. No coalescence of C_β proton or methyl resonances was observed. This bounds Δ*G*[‡]_{110°C} for Re=C=C isomerization in these compounds as ≥ 18 kcal/mol.

8. Photochemistry of Vinylidene Complexes. The (80 ± 2):(20 ± 2) equilibrium mixtures of *sc/ac* Re=C=C isomers of arylvinylidene complexes **3c-d**CF₃SO₃⁻ were irradiated with a Hanovia 450 W lamp (CD₂Cl₂, -78 °C). Analysis by ¹H NMR showed clean formation of (50 ± 2):(50 ± 2) photostationary states of *sc/ac* isomers. The samples were allowed to return to thermal equilibrium in the dark, and additional irradiation cycles were conducted without apparent sample deterioration.

9. Reactions of Vinylidene Complexes with Nucleophiles. We sought to determine whether the above vinylidene complexes underwent, like their alkylidene complex counterparts, stereospecific nucleophilic attack at C_α. First, dimethylvinylidene complex **7b**CF₃SO₃⁻ was prepared in situ from methyl acetylide complex **6b** and CF₃SO₃CH₃ and then treated with P(CH₃)₃. This gave the vinyl phosphonium salt [(η⁵-C₅H₅)Re(NO)(PPh₃)(C(P(CH₃)₃)=C(CH₃)₂)]⁺CF₃SO₃⁻ (**8**CF₃SO₃⁻) in 60% yield after recrystallization (Scheme IV).

A (98 ± 2):(2 ± 2) mixture of the *ac/sc* isomers of methylvinylidene complex **3b**CF₃SO₃⁻ was generated as described above and treated with P(CH₃)₃ at -78 °C (Scheme IV). This gave, as assayed by ¹H NMR at -80 °C, a (98 ± 2):(2 ± 2) mixture of vinyl phosphonium salts (*Z*)- and (*E*)-[(η⁵-C₅H₅)Re(NO)(PPh₃)(C(P(CH₃)₃)=CHCH₃)]⁺CF₃SO₃⁻ ((*Z*)- and (*E*)-**9**CF₃SO₃⁻; Scheme IV). Workup gave (*Z*)-**9**CF₃SO₃⁻ (³*J*_{PC=CH} = 36.3 Hz) in 57% yield. In a parallel experiment, a (95 ± 2):(5 ± 2) mixture of the *sc/ac* isomers of **3b**CF₃SO₃⁻ was generated by the low-temperature dissolution of a crystalline sample, as described above. Subsequent reaction with P(CH₃)₃ at -78 °C gave a (95 ± 2):(5 ± 2) mixture of (*E*)- and (*Z*)-**9**CF₃SO₃⁻. Workup gave (*E*)-**9**CF₃SO₃⁻ (³*J*_{PC=CH} = 60.7 Hz) in 80% yield. Neither (*Z*)- or (*E*)-**9**CF₃SO₃⁻ isomerized in CD₂Cl₂ (1 day, 22 °C). The (*Z*)/(*E*) assignments were made from previous observations that vinyl phosphonium salts, including related iron complexes [(η⁵-C₅H₅)Fe(CO)(PPh₃)(C(PPhR₂)=CH₂)]⁺, exhibit ³*J*_{PC=CHtrans} that are considerably greater than ³*J*_{PC=CHcis}.^{5b,29} These data establish that nucleophilic attack upon C_α of vinylidene complexes **3**CF₃SO₃⁻ occurs stereospecifically from a direction anti to the bulky PPh₃ ligand, as illustrated by transition state XIII in Scheme IV.

Discussion

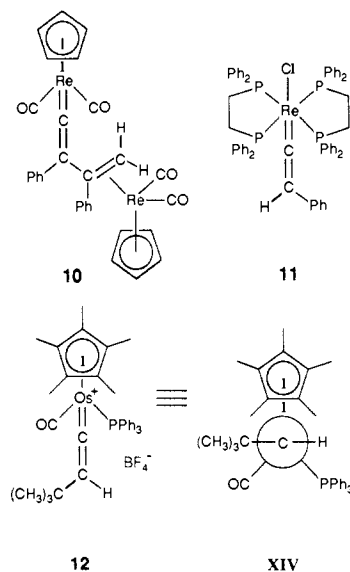
1. Vinylidene and Acetylide Complexes. Structure about Rhenium. It is interesting to compare the structures of na-

phthylvinylidene complex *sc*-**3d**PF₆⁻ and methyl acetylide complex **6b** to those of other [(η⁵-C₅H₅)Re(NO)(PPh₃)(X)]ⁿ⁺ complexes. First, both exhibit the ca. 90° P-Re-N, P-Re-C1, and N-Re-C1 bond angles noted earlier for this formally octahedral class of compounds (Tables V and IX).^{22a,23,24}

The Re=C_α double bond in naphthylvinylidene complex *sc*-**3d**PF₆⁻ (1.840 (17) Å) is, as expected, much shorter than the Re-C_α single bonds in alkyl complexes (-)(*R*)-(η⁵-C₅H₅)Re(NO)(PPh₃)(CH₂C₆H₅) (2.203 (8) Å)²³ and (*SS,RR*)-(η⁵-C₅H₅)Re(NO)(PPh₃)(CH(CH₂C₆H₅)C₆H₅) (2.215 (4) Å).^{22a} However, it is also somewhat shorter than the Re=C double bond in benzylidene complex [(η⁵-C₅H₅)Re(NO)(PPh₃)(=CHC₆H₅)]⁺PF₆⁻ (1.949 (6) Å).^{22a} This additional 5–6% contraction can be attributed to two factors. First, vinylidene ligands are superior π acids.^{20,30} Whereas alkylidene ligands have only a p acceptor orbital on C_α, vinylidene ligands have an additional, higher energy, π* acceptor orbital (Figure 4). In *sc*-**3d**PF₆⁻, the π* orbital would bond with an occupied d orbital that is of lower energy than, and orthogonal to, that shown in III.³⁰ Second, bonds to sp hybridized carbons (vinylidene C_α) are intrinsically shorter than those to sp² hybridized carbons (alkylidene C_α). For example, the C=C bond in allene (1.31 Å, sp²/sp) is contracted 2–3% from that in ethylene (1.34 Å, sp²/sp²).³¹

The Re-C_α single bond in methyl acetylide complex **6b** (2.066 (7) Å) is contracted 6–7% from those in analogous rhenium alkyl complexes. This also follows from the electronic and hybridization effects described above. However, Fenske, and Kostic have noted that both C_α acceptor orbitals in acetylide ligands (π*, π*) are of higher energy than those in vinylidene ligands and accordingly rank acetylide ligands as poor π acceptors.²⁰ Also, the H₃C-C bond in propyne (1.46 Å; sp³/sp) is shortened 5% from that in propane (1.54 Å; sp³/sp³).³¹ Hence, hybridization effects are likely responsible for most of the Re-C_α bond contraction in **6b**. Thus, acetylide complex resonance form II (eq 1) has a much greater influence upon ligand reactivity than structure.³²

2. Structures of Related Complexes. Although crystal structures of many vinylidene^{2,4,6b-d,8a,b,9b,10b,11,12b,c} and acetylide^{6c,18,19b-e} complexes have been determined, several are particularly relevant to this study. First, the structures of two other rhenium vinylidene complexes, (η⁵-C₅H₅)Re(CO)₂(=C=C(C₆H₅)R) (**10**) and



(29) Seyferth, D.; Fogel, J. J. *Organomet. Chem.* **1966**, *6*, 205.

(30) (a) Schilling, B. E. R.; Hoffmann, R.; Lichtenberger, D. L. *J. Am. Chem. Soc.* **1979**, *101*, 585. (b) Schilling, B. E. R.; Hoffmann, R.; Faller, J. W. *Ibid.* **1979**, *101*, 592.

(31) March, J. A. *Advanced Organic Chemistry*, 3rd ed.; Wiley: New York, 1985; pp 18–19.

(32) Yneamines are, like acetylide complexes **6**, nucleophilic at C_β, but none have been structurally characterized to our knowledge.²¹ It would be of interest to compare their sp³/sp nitrogen-carbon bond lengths with the sp³/sp² nitrogen-carbon bond lengths in saturated amines.

Table I. Spectroscopic Characterization of Rhenium Vinylidene Complexes

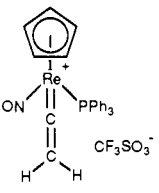
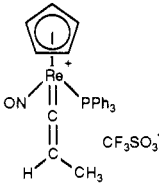
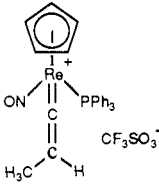
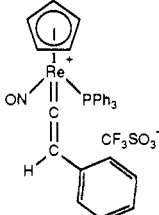
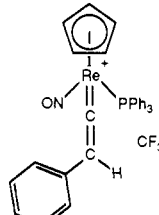
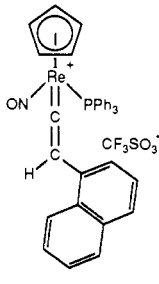
complex	IR ^a (cm ⁻¹)	¹ H NMR ^b (δ)	¹³ C{ ¹ H} NMR ^c (ppm)	³¹ P{ ¹ H} NMR ^d (ppm)
 3a CF ₃ SO ₃ ⁻	$\nu_{\text{N=O}}$ 1739 (s) $\nu_{\text{C=C}}$ 1641 (m)	7.60–7.20 (m, 3C ₆ H ₅) 6.02 (s, C ₅ H ₅) 5.50 (dd, ² J _{HH} = 20.0, ⁴ J _{HP} = 1.0, <i>sc</i> -H) 4.87 (dd, ² J _{HH} = 20.0, ⁴ J _{HP} = 1.4, <i>ac</i> -H)	329.9 (d, <i>J</i> = 9.9, C _α) 120.4 (q, <i>J</i> _{CF} = 319.6, CF ₃) 113.8 (s, C _β) 98.6 (s, C ₅ H ₅) PPh ₃ at: 132.9 (d, <i>J</i> = 11.5, <i>o</i>) 132.7 (d, <i>J</i> = 2.8, <i>p</i>) 129.7 (d, <i>J</i> = 11.8, <i>m</i>) 129.7 (d, <i>J</i> = 62.2, <i>i</i>)	17.0 (s)
 ac-3b CF ₃ SO ₃ ⁻	$\nu_{\text{N=O}}$ 1733 (s) $\nu_{\text{C=C}}$ 1664 (m)	7.90–7.25 (m, 3C ₆ H ₅) 6.19 (dq, ³ J _{HH} = 8.0, ⁴ J _{HP} = 1.0, =CH) 6.03 (s, C ₅ H ₅) 1.24 (d, ³ J _{HH} = 8.0, CH ₃)	328.5 (d, <i>J</i> = 10.1, C _α) 126.0 (s, C _β) 120.6 (q, <i>J</i> _{CF} = 319.9, CF ₃) 98.3 (s, C ₅ H ₅) 7.9 (s, CH ₃) PPh ₃ at: 133.0 (d, <i>J</i> = 10.7, <i>o</i>) 132.6 (s, <i>p</i>) 130.5 (d, <i>J</i> = 61.9, <i>i</i>) 129.7 (d, <i>J</i> = 9.8, <i>m</i>)	18.7 (s)
 sc-3b CF ₃ SO ₃ ⁻	$\nu_{\text{N=O}}$ 1733 (s) $\nu_{\text{C=C}}$ 1664 (m)	7.90–7.25 (m, 3C ₆ H ₅) 6.02 (s, C ₅ H ₅) 5.40 (dq, ³ J _{HH} = 7.8, ⁴ J _{HP} = 1.0, =CH) 1.91 (d, ³ J _{HH} = 7.8, CH ₃)	329.7 (d, <i>J</i> = 10.5, C _α) 125.3 (s, C _β) 120.6 (q, <i>J</i> _{CF} = 319.9, CF ₃) 98.5 (s, C ₅ H ₅) 10.0 (s, CH ₃) PPh ₃ at: 133.0 (d, <i>J</i> = 11.0, <i>o</i>) 132.6 (s, <i>p</i>) 129.8 (d, <i>J</i> = 64.0, <i>i</i>) 129.8 (d, <i>J</i> = 11.1, <i>m</i>)	18.3 (s)
 ac-3c CF ₃ SO ₃ ⁻	$\nu_{\text{N=O}}$ 1731 (s) $\nu_{\text{C=C}}$ 1651 (m)	7.75–7.20 (m, 3C ₆ H ₅) 7.02 (s, =CH) 7.01 (m, 1 H of C ₆ H ₅) 6.85 (t, <i>J</i> _{HH} = 7.7, 2 H of C ₆ H ₅) 6.50 (d, <i>J</i> _{HH} = 7.6, 2 H of C ₆ H ₅) 6.04 (s, C ₅ H ₅)	332.2 (d, <i>J</i> = 9.6, C _α) 124.6 (s, C _β) 120.4 (q, <i>J</i> _{CF} = 319.7, CF ₃) 98.9 (s, C ₅ H ₅) CPh at: 133.2 (s, <i>i</i>) 128.3 (s, <i>m</i>) 127.8 (s, <i>p</i>) 126.4 (s, <i>o</i>) PPh ₃ at: 133.0 (d, <i>J</i> = 10.6, <i>o</i>) 132.1 (s, <i>p</i>) 130.2 (d, <i>J</i> = 58.4, <i>i</i>) 129.2 (d, <i>J</i> = 11.0, <i>m</i>) ^e	18.3 (s)
 sc-3c CF ₃ SO ₃ ⁻	$\nu_{\text{N=O}}$ 1731 (s) $\nu_{\text{C=C}}$ 1651 (m)	7.75–7.20 (m, 4C ₆ H ₅) 6.14 (d, ⁴ J _{HP} = 1.4, =CH) 6.03 (s, C ₅ H ₅)	335.6 (d, <i>J</i> = 10.8, C _α) 127.0 (s, C _β) 120.6 (q, <i>J</i> _{CF} = 320.0, CF ₃) 98.9 (s, C ₅ H ₅) CPh at: 133.2 (s, <i>i</i>) 131.7 (s, <i>p</i>) 129.5 (s, <i>o</i>) 129.1 (s, <i>m</i>) PPh ₃ at: 133.0 (d, <i>J</i> = 11.4, <i>o</i>) 132.8 (d, <i>J</i> = 2.7, <i>p</i>) 129.8 (d, <i>J</i> = 11.8, <i>m</i>) 128.4 (d, <i>J</i> = 56.3, <i>i</i>)	17.0 (s)
 ac-3d CF ₃ SO ₃ ⁻	$\nu_{\text{N=O}}$ 1734 (s) $\nu_{\text{C=C}}$ 1641 (m)	7.90–7.17 (m, 3C ₆ H ₅ , 6 H of C ₁₀ H ₇ , =CH) 6.47 (d, <i>J</i> = 7.1, 1 H of C ₁₀ H ₇) 6.03 (s, C ₅ H ₅)	332.9 (d, <i>J</i> = 9.3, C _α) 120.2 (q, <i>J</i> _{CF} = 318.8, CF ₃) 98.6 (s, C ₅ H ₅) C ₁₀ H ₇ and C _β at: 133.9 (s), 132.8 (s), 132.2 (s) 127.9 (s), 127.5 (s), 127.1 (s) 126.1 (s), 126.0 (s), 126.0 (s) 125.4 (s), 124.5 (s) ^f PPh ₃ at: 132.5 (d, <i>J</i> = 17.0, <i>o</i>) 132.4 (s, <i>p</i>) 129.5 (d, <i>J</i> = 11.4, <i>m</i>) 129.2 (d, <i>J</i> = 62.3, <i>i</i>) ^g	16.8 (s)

Table I (Continued)

complex	IR ^a (cm ⁻¹)	¹ H NMR ^b (δ)	¹³ C{ ¹ H} NMR ^c (ppm)	³¹ P{ ¹ H} NMR ^d (ppm)
	$\nu_{\text{N=O}}$ 1734 (s) $\nu_{\text{C=C}}$ 1641 (m)	7.70–7.20 (m, 3C ₆ H ₅ , C ₁₀ H ₇) 6.83 (s, =CH) 6.02 (s, C ₅ H ₅)	336.3 (d, $J = 10.8$, C _α) 120.7 (q, J_{CF} = 320.5, CF ₃) 99.1 (s, C ₅ H ₅) C ₁₀ H ₇ and C _β at: 133.8 (s), 132.2 (s), 129.4 (s) 128.1 (s), 127.9 (s), 126.9 (s) 126.8 (s), 126.1 (s), 125.3 (s) 124.3 (s) ^{i,h} PPh ₃ at: 133.0 (d, $J = 11.5$, <i>o</i>) 132.8 (d, $J = 2.7$, <i>p</i>) 129.8 (d, $J = 11.7$, <i>m</i>) 129.4 (d, $J = 62.4$, <i>i</i>)	16.6 (s)
sc-3d CF ₃ SO ₃ ⁻	$\nu_{\text{N=O}}$ 1748 (s) $\nu_{\text{C=C}}$ 1654 (m) ⁱ	7.62–7.32 (m, 3C ₆ H ₅) 6.02 (s, C ₅ H ₅) 1.96 (s, <i>sc</i> -CH ₃) 1.24 (s, <i>ac</i> -CH ₃)	327.9 (d, $J = 11.1$, C _α) 136.8 (s, C _β) 98.2 (s, C ₅ H ₅) 17.5 (s, <i>sc</i> -CH ₃) 13.8 (s, <i>ac</i> -CH ₃) PPh ₃ at: 133.2 (s, <i>p</i>) 132.8 (d, $J = 18.9$, <i>o</i>) 131.1 (d, <i>i</i>) ^y 129.8 (d, $J = 12.8$, <i>m</i>)	18.4 (s)
7b FSO ₃ ⁻				

^aThin film unless noted; $\nu_{\text{N=O}}$ and $\nu_{\text{C=C}}$ for **3b-d** were assigned from spectra of equilibrium mixtures. ^b¹H NMR spectra were recorded at 200 or 300 MHz in CDCl₃ at ambient probe temperature and were referenced to internal (CH₃)₄Si. All couplings are in Hz. ^c¹³C NMR spectra were recorded at 50 or 75 MHz in CDCl₃ at ambient probe temperature and were referenced to internal (CH₃)₄Si unless noted. All couplings are in Hz and are to ³¹P unless noted. Assignments of ipso (*i*), para (*p*), meta (*m*), and ortho (*o*) carbon resonances were made as described in footnote c of Table I in the following: Buhro, W. E.; Georgiou, S.; Fernández, J. M.; Patton, A. T.; Strouse, C. E.; Gladysz, J. A. *Organometallics* **1986**, *5*, 956. ^d³¹P NMR spectra were recorded at 32 MHz in CDCl₃ at ambient temperature with an external lock and were referenced to external 85% H₃PO₄. ^eIn CD₂Cl₂ at -80 °C. ^fC_β resonance cannot be distinguished from the naphthyl resonances. ^gAt 0 °C. ^hOne resonance obscured by PPh₃ resonances. ⁱIn CHCl₃. ^jUpfield resonance of doublet obscured.

Table II. Summary of Crystallographic Data for *sc*-[(η⁵-C₅H₅)Re(NO)(PPh₃)(=C=CH(1-C₁₀H₇))]PF₆⁻ (**sc-3dPF₆⁻**) and (η⁵-C₅H₅)Re(NO)(PPh₃)(C≡CCH₃) (**6b**)

compd	<i>sc-3dPF₆⁻</i>	6b
mol formula	C ₃₅ H ₂₈ F ₆ NOP ₂ Re	C ₂₆ H ₂₃ NOPRe
formula wt	840.76	582.66
cryst system	monoclinic	triclinic
space group	<i>C2/c</i>	<i>P</i> $\bar{1}$
cell dimensions		
<i>a</i> , Å	25.768 (8)	8.055 (4)
<i>b</i> , Å	11.215 (3)	16.419 (10)
<i>c</i> , Å	23.475 (8)	9.084 (5)
α , deg		91.46 (5)
β , deg	104.08 (3)	68.57 (4)
γ , deg		77.36 (4)
<i>V</i> , Å ³	6580 (4)	1095.6 (8)
<i>Z</i>	8	2
temp of collectn	21 (1) °C	-158 (5) °C
<i>d</i> _{calcd} , g/cm ³	1.70	1.78
<i>d</i> _{obsd} , g/cm ³ (22 °C)	1.71	1.79
cryst dimensions, mm	0.19 × 0.24 × 0.24	0.14 × 0.16 × 0.18
radiation, Å	λ (Mo Kα) 0.71069	λ (Mo Kα) 0.71069
data collectn method	θ-2θ	θ-2θ
scan speed, deg/min ⁻¹	2.4	6.0
reflcs measd	+ <i>h</i> , + <i>k</i> , ± <i>l</i> ; 3-50°	+ <i>h</i> , ± <i>k</i> , ± <i>l</i> ; 3-50°
scan range	Kα ₁ - 1.0 to Kα ₂ + 1.3	Kα ₁ - 1.0 to Kα ₂ + 1.0
no. of reflcs between std	97	97
total unique data	5828	3975
cutoff for obsd data	<i>I</i> > 1.5σ(<i>I</i>)	<i>I</i> > 3.0σ(<i>I</i>)
obsd data	4197	3852
abs coeff (μ), cm ⁻¹	39.00	55.32
method of refinement	full matrix least squares	full matrix least squares
no. of variables	420	266
<i>R</i> = Σ(<i>F</i> _o - <i>F</i> _c)/Σ <i>F</i> _o	0.063	0.041
<i>R</i> _w = Σ(<i>F</i> _o - <i>F</i> _c)w ^{1/2} /Σ <i>F</i> _o w ^{1/2}	0.054	0.051
goodness of fit	1.43	1.75
weighting factor, <i>w</i>	1/(σ ² (<i>F</i> _o) + 0.0016(<i>F</i> _o) ²)	1/(σ ² (<i>F</i> _o) + 0.0045(<i>F</i> _o) ²)

trans-(dppe)₂Re(Cl)(=C=CHC₆H₅) (**11**),^{27c} have been reported.¹¹ They exhibit longer Re=C_α bonds (1.90 (2), 2.046 (8) Å)

than *sc-3dPF₆⁻* (1.840 (17) Å). This can be attributed to the greater π basicity of the (η⁵-C₅H₅)Re(NO)(PPh₃)⁺ fragment. Osmium *tert*-butylvinylidene complex [(η⁵-C₅Me₅)Os(CO)(PPh₃)(=C=CH(*t*-C₄H₉))]BF₄⁻ (**12**), which is isoelectronic with **3a-dCF₃SO₃⁻**, has been prepared by Geoffroy.^{10b} It has a M=C_α bond length (1.879 (6) Å) closer to that of *sc-3dPF₆⁻*.

The alkylidene/vinylidene Re=C_α bond contraction noted above has precedent. For example, the Mn=C_α bond in manganese vinylidene complex (η⁵-C₅H₅)Mn(CO)₂(=C=C(CH₃)₂) (1.79 (2) Å)^{13c} is shorter than that in alkylidene complex (η⁵-C₅H₅)Mn(CO)₂(=C(C₆H₅)₂) (1.885 (2) Å).³³ Similarly, the Ru=C_α bonds in ruthenium vinylidene complexes [(η⁵-C₅H₅)Ru(L)₂(=C=CRCH₃)]⁺X⁻ (L = phosphine; R = H, C₆H₅; 1.839 (10)-1.863 (10) Å) are shorter than those in α-methoxycarbene complexes [(η⁵-C₅H₅)Ru(L)₂(=C(OCH₃)CH₂R)]⁺PF₆⁻ (1.93 (2)-1.959 (6) Å).^{6c,9b}

To our knowledge, **6d** is the only structurally characterized rhenium acetylide complex. However, the structure of an acetylide complex of a neighboring third-row metal, (η⁵-C₅H₅)W(CO)₂(P(CH₃)₃)(C≡C(*i*-C₃H₇)), has been reported (W-C_α 2.134 (11) Å).^{19b} This complex and **6b** have C≡C bond lengths (1.205 (15), 1.192 (11) Å) identical with those in organic acetylenes (1.20 Å).³¹ Although longer C≡C bonds might be expected in acetylide complexes as a result of resonance form II, it is believed that the lengths of bonds of bond order between two and three are not very sensitive to small changes in bond order.³⁴

3. M=C=C Isomerization in Vinylidene Complexes. Several factors made it difficult to obtain accurate rate data for vinylidene complex Re=C=C isomerizations over a wide range of temperatures (Table X-A). However, the available data show Δ*G*[‡] (21 °C) to be relatively constant, with the Δ*H*[‡] increase for *ac-3/c/d*/bCF₃SO₃⁻ → *sc-3/c/d*/bCF₃SO₃⁻ offset by a Δ*S*[‡] increase (Table X-B). This suggests an isokinetic relationship,³⁵ with an isokinetic temperature of 124 °C. Such behavior is associated with a common rate-determining step and has been observed previously for *cis/trans* isomerizations of stilbenes and

(33) Herrmann, W. A.; Hubbard, J. L.; Bernal, I.; Korp, J. D.; Haymore, B. L.; Hillhouse, G. L. *Inorg. Chem.* **1984**, *23*, 2978.

(34) Cotton, F. A.; Wing, R. M. *Inorg. Chem.* **1965**, *4*, 314.

Table III. Atomic Coordinates of Non-Hydrogen Atoms in $sc\text{-}[(\eta^5\text{-C}_5\text{H}_5)\text{Re}(\text{NO})(\text{PPh}_3)(=\text{C}=\text{CH}(\text{1-C}_{10}\text{H}_7))]\text{PF}_6^- (sc\text{-}3d\text{PF}_6^-)$

atom	x	y	z
Re	0.143 380 (15)	0.070 09 (4)	0.220 330 (19)
P1	0.080 13 (9)	0.042 61 (22)	0.126 89 (11)
O	0.057 19 (35)	0.132 08 (85)	0.276 85 (41)
N	0.091 77 (36)	0.104 12 (73)	0.253 25 (38)
C1	0.142 80 (37)	-0.092 19 (150)	0.231 63 (41)
C2	0.140 55 (46)	-0.214 50 (110)	0.239 58 (53)
C11	0.159 65 (39)	-0.269 03 (97)	0.300 02 (50)
C12	0.192 57 (42)	-0.212 68 (102)	0.345 67 (52)
C13	0.210 71 (42)	-0.262 86 (112)	0.401 31 (48)
C14	0.195 41 (48)	-0.377 08 (124)	0.411 06 (51)
C16	0.108 82 (83)	-0.612 94 (145)	0.329 59 (88)
C15	0.142 81 (74)	-0.554 99 (130)	0.373 17 (66)
C17	0.089 61 (69)	-0.562 92 (143)	0.274 12 (70)
C18	0.105 42 (54)	-0.450 71 (118)	0.262 69 (63)
C19	0.142 17 (41)	-0.384 92 (100)	0.308 10 (54)
C20	0.160 83 (46)	-0.440 23 (103)	0.364 10 (54)
C31	0.235 03 (37)	0.077 51 (130)	0.255 69 (63)
C32	0.223 68 (42)	0.074 73 (128)	0.195 69 (56)
C33	0.196 99 (46)	0.180 96 (162)	0.173 04 (59)
C34	0.191 09 (43)	0.251 04 (112)	0.222 00 (77)
C35	0.213 42 (49)	0.183 01 (130)	0.274 11 (55)
C41	0.114 49 (38)	0.020 06 (93)	0.068 76 (42)
C42	0.150 07 (40)	-0.072 72 (99)	0.071 69 (47)
C43	0.179 53 (46)	-0.088 03 (110)	0.028 98 (58)
C44	0.169 49 (58)	-0.006 70 (136)	-0.018 22 (57)
C45	0.132 55 (51)	0.084 35 (132)	-0.022 04 (53)
C46	0.105 25 (42)	0.097 51 (106)	0.021 22 (50)
C52	-0.018 34 (38)	0.153 29 (94)	0.076 98 (43)
C51	0.035 24 (35)	0.168 31 (86)	0.105 03 (42)
C53	-0.050 55 (41)	0.252 20 (111)	0.058 69 (48)
C54	-0.029 53 (51)	0.364 39 (115)	0.067 03 (54)
C55	0.023 39 (54)	0.381 51 (114)	0.094 61 (68)
C56	0.055 90 (42)	0.283 10 (105)	0.113 31 (55)
C61	0.036 27 (33)	-0.086 51 (87)	0.125 13 (42)
C62	0.006 00 (39)	-0.093 88 (99)	0.166 97 (46)
C63	-0.026 88 (41)	-0.189 59 (116)	0.167 34 (52)
C64	-0.029 41 (44)	-0.282 05 (103)	0.127 51 (59)
C65	0.000 45 (49)	-0.274 19 (98)	0.086 16 (51)
C66	0.033 99 (43)	-0.177 25 (96)	0.086 15 (48)
P2	0.170 07 (14)	-0.542 68 (30)	0.580 33 (15)
F1	0.113 59 (41)	-0.590 44 (142)	0.567 00 (64)
F2	0.187 58 (52)	-0.657 82 (83)	0.616 38 (41)
F3	0.228 66 (42)	-0.511 56 (140)	0.597 02 (66)
F4	0.152 87 (74)	-0.426 87 (98)	0.546 66 (48)
F5	0.163 54 (46)	-0.478 26 (90)	0.636 83 (38)
F6	0.176 30 (53)	-0.604 02 (97)	0.523 52 (38)

Table IV. Bond Distances in $sc\text{-}3d\text{PF}_6^-$ (Å)

Re-C1	1.840 (17)	C32-C33	1.413 (18)
C1-C2	1.387 (17)	C33-C34	1.431 (18)
C2-C11	1.513 (15)	C34-C35	1.438 (17)
Re-N	1.735 (9)	C41-C42	1.377 (14)
N-O	1.200 (10)	C41-C46	1.388 (13)
Re-C31	2.306 (9)	C42-C43	1.408 (14)
Re-C32	2.281 (11)	C43-C44	1.410 (17)
Re-C33	2.331 (12)	C44-C45	1.384 (18)
Re-C34	2.368 (11)	C45-C46	1.377 (15)
Re-C35	2.312 (11)	C51-C52	1.388 (12)
Re-P1	2.413 (3)	C51-C56	1.389 (14)
P1-C41	1.816 (10)	C52-C53	1.389 (14)
P1-C51	1.817 (9)	C53-C54	1.365 (16)
P1-C61	1.831 (9)	C54-C55	1.373 (16)
C11-C12	1.351 (14)	C55-C56	1.391 (15)
C11-C19	1.403 (14)	C61-C66	1.360 (13)
C12-C13	1.394 (14)	C61-C62	1.397 (12)
C13-C14	1.376 (16)	C62-C63	1.369 (14)
C14-C20	1.426 (16)	C63-C64	1.387 (15)
C15-C16	1.342 (21)	C64-C65	1.380 (15)
C15-C20	1.402 (17)	C65-C66	1.389 (14)
C16-C17	1.393 (22)	P2-F1	1.510 (10)
C17-C18	1.369 (17)	P2-F2	1.550 (10)
C18-C19	1.444 (17)	P2-F3	1.506 (10)
C19-C20	1.427 (15)	P2-F4	1.529 (10)
C31-C32	1.367 (16)	P2-F5	1.555 (9)
C31-C35	1.419 (17)	P2-F6	1.543 (9)

Table V. Key Bond Angles in $sc\text{-}3d\text{PF}_6^-$ (deg)

N-Re-P1	90.7 (3)	Re-P1-C51	113.6 (3)
C1-Re-P1	88.7 (3)	Re-P1-C61	113.5 (3)
C1-Re-N	96.9 (4)	C32-C31-C35	109.4 (12)
Re-C1-C2	178.1 (9)	C31-C32-C33	109.3 (13)
Re-N-O	177.2 (8)	C32-C33-C34	107.3 (12)
C1-Re-C31	91.6 (5)	C33-C34-C35	107.0 (12)
C1-Re-C32	95.7 (5)	C31-C35-C34	106.8 (12)
C1-Re-C33	128.5 (5)	C42-C41-C46	119.6 (10)
C1-Re-C34	150.2 (4)	P1-C41-C42	120.5 (8)
C1-Re-C35	119.7 (5)	P1-C41-C46	119.8 (8)
C1-C2-C11	120.7 (12)	C41-C42-C43	121.6 (10)
C12-C11-C19	119.1 (11)	C42-C43-C44	117.0 (11)
C12-C11-C2	123.6 (11)	C45-C44-C43	121.3 (11)
C19-C11-C2	117.3 (11)	C46-C45-C44	119.9 (11)
C11-C12-C13	123.8 (11)	C45-C46-C41	120.5 (11)
C14-C13-C12	119.2 (11)	C52-C51-C56	118.8 (9)
C13-C14-C20	119.0 (11)	P1-C51-C52	122.1 (8)
C16-C15-C20	120.5 (14)	P1-C51-C56	118.9 (7)
C15-C16-C17	122.3 (15)	C51-C52-C53	120.0 (10)
C18-C17-C16	119.9 (15)	C54-C53-C52	120.4 (10)
C17-C18-C19	119.8 (14)	C53-C54-C55	120.7 (11)
C11-C19-C20	118.7 (11)	C54-C55-C56	119.4 (12)
C11-C19-C18	123.2 (12)	C51-C56-C55	120.7 (10)
C20-C19-C18	118.1 (11)	C66-C61-C62	119.2 (9)
C15-C20-C14	120.4 (13)	P1-C61-C66	122.2 (7)
C15-C20-C19	119.3 (13)	P1-C61-C62	118.6 (8)
C14-C20-C19	120.2 (11)	C63-C62-C61	120.2 (10)
C41-P1-C51	106.8 (5)	C62-C63-C64	120.6 (10)
C41-P1-C61	106.5 (5)	C65-C64-C63	118.9 (10)
C51-P1-C61	105.1 (4)	C64-C65-C66	120.2 (10)
Re-P1-C41	110.8 (3)	C61-C66-C65	120.7 (9)

azo compounds.^{35a} However, few examples of isokinetic relationships are known in inorganic and organometallic reactions.^{35b}

Interestingly, the activation parameters for $sc \rightarrow ac$ $\text{Re}=\text{C}$ isomerization of alkylidene complexes $[(\eta^5\text{-C}_5\text{H}_5)\text{Re}(\text{NO})(\text{PPh}_3)(=\text{CHR})]\text{PF}_6^-$ (IV \rightarrow V, Figure 1b; R = C_6H_5 ,^{22a} CH_3 ,^{22b} mesityl;^{22c} $\Delta H^\ddagger = 20.9, 17.4, 18.8$ kcal/mol; $\Delta S^\ddagger = -3.8, -7.3, 0.5$ eu) are quite close to those for $ac \rightarrow sc$ $\text{Re}=\text{C}=\text{C}$ isomerization in Table X.³⁶ This is in one sense surprising, since the $=\text{CRR}'$ π terminus is farther from the metal in vinylidene complexes. This should reduce the steric component of the isomerization barrier.³⁷ Hence, there is likely a greater electronic component of the isomerization barrier in vinylidene complexes. Unfortunately, this is impossible to ascribe to a single factor, since the extra $\text{C}_\alpha=\text{C}_\beta$ unsaturation in vinylidene complexes creates a complex array of conformation-dependent attractive and repulsive metal/ C_α orbital interactions.^{20,30}

The K_{eq} for $sc \rightleftharpoons ac$ $\text{Re}=\text{C}$ isomerization in alkylidene complexes $[(\eta^5\text{-C}_5\text{H}_5)\text{Re}(\text{NO})(\text{PPh}_3)(=\text{CHR})]\text{PF}_6^-$ (R = CH_3 ,^{22b} C_6H_5 ,^{22a} $K_{\text{eq}} = 9.0 \pm 1.0, \geq 99$) are, however, considerably greater than those for $ac \rightleftharpoons sc$ $\text{Re}=\text{C}=\text{C}$ isomerization in Table X. This can be attributed to the larger metal/ $=\text{CRR}'$ separation in vinylidene complexes. Also, photolysis of ac/sc equilibrium mixtures of alkylidene complexes $[(\eta^5\text{-C}_5\text{H}_5)\text{Re}(\text{NO})(\text{PPh}_3)(=\text{CHR})]\text{PF}_6^-$ (R = CH_2CH_3 ,³⁸ C_6H_5 ,^{22a} mesityl^{22c}) gives, as with vinylidene complexes $3c\text{-dCF}_3\text{SO}_3^-$, ca. 50:50 sc/ac photostationary states. This suggests similar initial metal-to-ligand charge-transfer (MLCT) transitions to give excited states with formal $\text{Re}-\text{C}_\alpha$ single bonds.³⁹

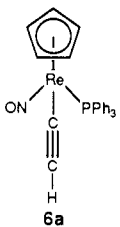
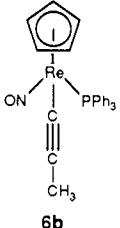
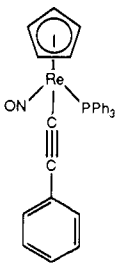
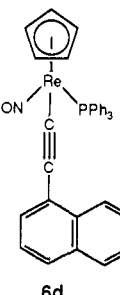
(35) (a) Leffler, J. E.; Grunwald, E. *Rates and Equilibria of Organic Reactions*; Wiley: New York, 1963; Chapter 9. (b) Wilkins, R. G. *The Study of Kinetics and Mechanism of Reactions of Transition Metal Complexes*; Allyn and Bacon: Boston, 1974; pp 100-101. (c) Giese, B. *Acc. Chem. Res.* **1984**, *17*, 438. (d) Linert, W. *Inorg. Chim. Acta* **1988**, *141*, 233.

(36) (a) None of our data rigorously establish whether vinylidene complex $\text{Re}=\text{C}=\text{C}$ isomerization occurs via $\text{Re}=\text{C}_\alpha$ or $\text{C}_\alpha=\text{C}_\beta$ bond rotation. However, since the barriers are similar to those for $\text{Re}=\text{C}_\alpha$ isomerization in the corresponding alkylidene complexes, and alkene $\text{C}=\text{C}$ rotation normally requires much higher temperatures,^{36b} we assume that $\text{Re}=\text{C}_\alpha$ bond rotation is occurring. (b) Gajewski, J. J. *Hydrocarbon Thermal Isomerization*; Academic Press: New York, 1981; pp 17-18.

(37) Further, since a vinylidene substituent is directed at the bulky PPh_3 ligand in the $\text{Re}=\text{C}=\text{C}$ ground states, steric interactions may be attenuated in the $\text{Re}=\text{C}=\text{C}$ isomerization transition states.

(38) McCormick, F. B.; Kiel, W. A.; Gladysz, J. A. *Organometallics* **1982**, *1*, 405.

Table VI. Spectroscopic Characterization of Rhenium Acetylide Complexes

complex	IR ^a (cm ⁻¹)	¹ H NMR ^b (δ)	¹³ C{ ¹ H} NMR (ppm)	³¹ P{ ¹ H} ^d NMR (ppm)
	$\nu_{\text{N=O}}$ 1654 (s) $\nu_{\text{C=C}}$ 1947 (w) $\nu_{\text{=CH}}$ 3282 (m)	7.60–7.30 (m, 3C ₆ H ₅) 5.11 (s, C ₅ H ₅) 2.53 (d, ⁴ J _{HP} = 2.4, ≡CH)	111.7 (s, C _β) 90.4 (s, C ₅ H ₅) 84.5 (d, J = 15.4, C _α) PPh ₃ at: 135.3 (d, J = 60.0, i) 133.7 (d, J = 8.8, o) 130.3 (s, p) 128.1 (d, J = 8.0, m)	18.9 (s)
	$\nu_{\text{N=O}}$ 1650 (s) $\nu_{\text{C=C}}$ 2113 (w)	7.72–7.38 (m, 3C ₆ H ₅) 5.13 (s, C ₅ H ₅) 2.05 (d, ⁵ J _{HP} = 3.0, CH ₃)	120.7 (s, C _β) 90.1 (s, C ₅ H ₅) 71.7 (d, J = 17.0, C _α) 6.5 (s, CH ₃) PPh ₃ at: 135.6 (d, J = 55.0, i) 133.9 (d, J = 14.6, o) 130.1 (d, p) 128.4 (d, J = 12.2, m)	20.2 (s)
	$\nu_{\text{N=O}}$ 1652 (s) $\nu_{\text{C=C}}$ 2082 (w)	7.60–7.12 (m, 3C ₆ H ₅) 6.92–6.71 (m, C ₆ H ₅) 5.24 (s, C ₅ H ₅)	122.8 (s, C _β) 92.3 (d, J = 22.1, C _α) 90.6 (s, C ₅ H ₅) CPh at: 136.7 (s, i) 131.0 (s, o) 127.4 (s, m) 124.6 (s, p) PPh ₃ at: 135.5 (d, J = 52.6, i) 133.8 (d, J = 10.6, o) 130.2 (s, p) 128.3 (d, J = 10.8, m)	19.1 (s)
	$\nu_{\text{N=O}}$ 1657 (s) $\nu_{\text{C=C}}$ 2067 (w)	8.00 (m, 1 H of C ₁₀ H ₇) 7.70 (m, 1 H of C ₁₀ H ₇) 7.64–7.22 (m, 3C ₆ H ₅ , 4H of C ₁₀ H ₇) 6.96 (m, 1 H of C ₁₀ H ₇) 5.29 (s, C ₅ H ₅)	124.2 (s, C _β) 98.3 (d, J = 17.0, C _α) 90.6 (s, C ₅ H ₅) C ₁₀ H ₇ at: 133.0 (s), 132.8 (s) 127.9 (s), 127.4 (s) 127.0 (s), 125.8 (s) 125.2 (s), 125.1 (s) 125.0 (s), 124.9 (s) PPh ₃ at: 135.3 (d, J = 52.8, i) 133.5 (d, J = 9.8, o) 130.0 (d, J = 2.5, p) 128.1 (d, J = 11.0, m)	18.8 (s)

^aThin film. ^b¹H NMR spectra were recorded at 300 MHz in CDCl₃ at ambient probe temperature and were referenced to internal (CH₃)₄Si. All couplings are in Hz. ^c¹³C NMR spectra were recorded at 50 or 75 MHz in CDCl₃ at ambient probe temperature and were referenced to internal (CH₃)₄Si. All couplings are in Hz and are to ³¹P. Assignments of ipso (*i*), para (*p*), meta (*m*), and ortho (*o*) carbon resonances were made as described in footnote c of Table I in the following: Buhro, W. E.; Georgiou, S.; Fernández, J. M.; Patton, A. T.; Strouse, C. E.; Gladysz, J. A. *Organometallics* **1986**, *5*, 956. ^d³¹P NMR spectra were recorded at 32 MHz in CDCl₃ at ambient probe temperature with an external lock and were referenced to external 85% H₃PO₄.

Several results from other laboratories are particularly relevant to our data. First, Consiglio has recently observed M=C=C isomerism in iron and ruthenium vinylidene complexes [(η^5 -C₅H₅)M(L)₂(=C=CHR)]⁺PF₆⁻ (L = 1/2 chiral diphosphine).^{9a,c,d} Depending upon substituents, *K*_{eq} range from 1.0 to ≥ 9.0 , and dynamic NMR experiments give $\Delta G^\ddagger = 9$ –10 kcal/mol for M=C=C isomerization. Second, Hughes has placed an upper limit of $\Delta G^\ddagger_{-100^\circ\text{C}} = 8$ –9 kcal/mol for Fe=C=C isomerization in dimethylvinylidene complex [(η^5 -C₅H₅)Fe(CO)(PPh₃)(=C=C(CH₃)₂)]⁺CF₃SO₃⁻.^{5b} This compound is analogous to rhenium complex **7b**FSO₃⁻, and the iron fragment (η^5 -C₅H₅)Fe(CO)(PPh₃)⁺ should have a HOMO similar to that of rhenium fragment (η^5 -C₅H₅)Re(NO)(PPh₃)⁺ (see III).³⁰ Hence, the electronic component of the M=C=C isomerization barrier is much lower in the iron vinylidene complex.

The osmium fragment (η^5 -C₅Me₅)Os(CO)(PPh₃)⁺ is also expected to have a HOMO similar to that shown in III.³⁰ However,

the *tert*-butylvinylidene ligand in the corresponding complex **12** adopts the Os=C=C conformation shown in Newman projection XIV. The Ph₃P–M–C_β–C torsion angle differs from that in *sc*-**3d**PF₆⁻ (Figure 2, bottom) by ca. 27°. Geoffroy has suggested that the greater bulk of the pentamethylcyclopentadienyl ligand magnifies steric conformation determining factors. This would direct the *tert*-butyl substituent toward the smaller CO ligand at the expense of some metal HOMO/C_α p orbital overlap. We agree with this analysis and also predict that low-temperature photolysis of **12** may allow detection of a second Os=C=C isomer.

4. Reactivity of Vinylidene and Acetylide Complexes. Mechanism of Asymmetric Induction. The reaction polarity of vinylidene and acetylide ligands was first systematically studied by Davison and Selegue.^{3a,c} They found that iron vinylidene and acetylide complexes [(η^5 -C₅H₅)Fe(L)₂(X)]ⁿ⁺ exhibit significant C_α electrophilicity and C_β nucleophilicity, respectively. The related rhenium complexes **3a–d**CF₃SO₃⁻ and **6a–d** behave similarly. This reactivity has been probed theoretically by Fenske and Kostić.²³ They attribute the vinylidene ligand C_α electrophilicity to the LUMO character and localization and the acetylide ligand C_β

(39) (a) Pourreau, D. B.; Geoffroy, G. L. *Adv. Organomet. Chem.* **1985**, *24*, 249. (b) The long wavelength UV absorptions of **3d**CF₃SO₃⁻ are also likely due to MLCT transitions.^{39a}

Table VII. Atomic Coordinates of Non-Hydrogen Atoms in $(\eta^5\text{-C}_5\text{H}_5)\text{Re}(\text{NO})(\text{PPh}_3)(\text{C}\equiv\text{CCH}_3)$ (**6b**)

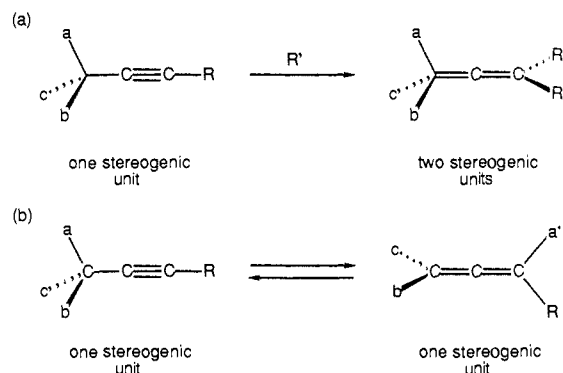
atom	x	y	z
Re	-0.66726 (4)	-0.16493 (3)	-0.33533 (4)
P1	-0.5895 (2)	-0.2358 (1)	-0.1356 (2)
O	-0.3138 (7)	-0.1150 (3)	-0.4702 (7)
N	-0.4538 (8)	-0.1388 (4)	-0.4129 (8)
C1	-0.5901 (10)	-0.2813 (5)	-0.4637 (9)
C2	-0.5524 (11)	-0.3463 (5)	-0.5441 (10)
C3	-0.5072 (13)	-0.4244 (6)	-0.6514 (12)
C11	-0.9625 (11)	-0.1032 (7)	-0.1555 (11)
C12	-0.8917 (13)	-0.0400 (6)	-0.2342 (14)
C13	-0.8568 (12)	-0.0574 (7)	-0.3963 (13)
C14	-0.9060 (14)	-0.1307 (6)	-0.4188 (12)
C15	-0.9734 (11)	-0.1604 (6)	-0.2687 (14)
C21	-0.3885 (10)	-0.3259 (5)	-0.2023 (9)
C22	-0.3921 (11)	-0.4031 (5)	-0.1399 (11)
C23	-0.2335 (12)	-0.4679 (5)	-0.1908 (12)
C24	-0.0702 (12)	-0.4554 (6)	-0.3032 (11)
C25	-0.0653 (11)	-0.3793 (6)	-0.3633 (10)
C26	-0.2245 (11)	-0.3146 (5)	-0.3152 (9)
C31	-0.5414 (9)	-0.1703 (5)	0.0035 (8)
C32	-0.6395 (11)	-0.0880 (5)	0.0490 (10)
C33	-0.6160 (12)	-0.0380 (5)	0.1631 (11)
C34	-0.4911 (10)	-0.0707 (5)	0.2300 (9)
C35	-0.3911 (11)	-0.1520 (5)	0.1845 (10)
C36	-0.4144 (11)	-0.2032 (5)	0.0707 (10)
C41	-0.7761 (10)	-0.2779 (5)	-0.0021 (9)
C42	-0.8532 (10)	-0.3298 (5)	-0.0685 (10)
C43	-1.0003 (11)	-0.3595 (5)	0.0309 (11)
C44	-1.0728 (11)	-0.3358 (5)	0.1948 (11)
C45	-0.9953 (12)	-0.2858 (6)	0.2589 (11)
C46	-0.8457 (11)	-0.2566 (5)	0.1612 (10)

Table VIII. Bond Distances in **6b** (Å)

Re-C1	2.066 (7)	C22-C23	1.388 (11)
C1-C2	1.192 (11)	C23-C24	1.401 (13)
C2-C3	1.484 (12)	C24-C25	1.380 (13)
Re-N	1.758 (6)	C25-C26	1.391 (11)
N-O	1.212 (8)	P1-C31	1.837 (7)
Re-C11	2.313 (8)	C31-C32	1.373 (10)
Re-C12	2.319 (9)	C31-C36	1.394 (10)
Re-C13	2.299 (8)	C32-C33	1.398 (11)
Re-C14	2.293 (10)	C33-C34	1.377 (11)
Re-C15	2.300 (8)	C34-C35	1.363 (11)
C11-C12	1.383 (15)	C35-C36	1.407 (11)
C11-C15	1.413 (14)	P1-C41	1.836 (7)
C12-C13	1.404 (16)	C41-C46	1.385 (11)
C13-C14	1.378 (15)	C41-C42	1.398 (11)
C14-C15	1.415 (15)	C42-C43	1.396 (11)
Re-P1	2.362 (2)	C43-C44	1.395 (13)
P1-C21	1.835 (7)	C44-C45	1.367 (13)
C21-C26	1.399 (11)	C45-C46	1.400 (12)
C21-C22	1.403 (11)		

Table IX. Bond Angles in **6b** (deg)

N-Re-P1	92.5 (2)	Re-P1-C31	115.1 (2)
C1-Re-P1	87.0 (2)	P1-C31-C32	119.3 (5)
C1-Re-N	97.7 (3)	P1-C31-C36	121.6 (6)
Re-C1-C2	175.8 (7)	C32-C31-C36	119.0 (7)
C1-C2-C3	176.8 (9)	C31-C32-C33	121.0 (7)
Re-N-O	175.0 (6)	C34-C33-C32	120.0 (7)
C1-Re-C14	88.0 (3)	C35-C34-C33	119.7 (7)
C12-C11-C15	108.0 (9)	C34-C35-C36	120.9 (7)
C11-C12-C13	108.0 (9)	C31-C36-C35	119.4 (7)
C14-C13-C12	109.0 (8)	Re-P1-C41	112.9 (2)
C13-C14-C15	107.6 (9)	P1-C41-C46	121.4 (6)
C11-C15-C14	107.4 (8)	P1-C41-C42	118.8 (6)
Re-P1-C21	117.6 (2)	C46-C41-C42	119.8 (7)
P1-C1-C26	117.6 (6)	C43-C42-C41	119.6 (7)
P1-C21-C22	122.7 (6)	C44-C43-C42	120.2 (8)
C26-C21-C22	119.7 (7)	C45-C44-C43	119.8 (8)
C23-C22-C21	119.9 (8)	C44-C45-C46	120.7 (8)
C22-C23-C24	119.6 (8)	C41-C46-C45	119.9 (8)
C25-C24-C23	120.7 (7)	C21-P1-C41	104.1 (4)
C24-C25-C26	120.0 (8)	C21-P1-C31	102.8 (3)
C25-C26-C21	120.0 (8)	C41-P1-C31	102.6 (3)

**Figure 5.** Schematic comparison of the stereochemistry of (a) electrophilic attack upon acetylide complexes **6b-d** (Schemes II-III) with (b) that of interconverting propargyl and allenic systems.

nucleophilicity to charge distribution (eq 1). Also, the $\text{p}K_{\text{b}}$ of $(\eta^5\text{-C}_5\text{H}_5)\text{Fe}(\text{dppe})(\text{C}\equiv\text{CCH}_3)$ is ca. 6.26 (2:1 THF/ H_2O),^{3a} which shows that acetylide complexes can be moderately strong bases.

The stereospecificity observed in the reactions of acetylide complexes **6b-d** with electrophiles is easily rationalized. First, note the four acetylide C_β p orbital lobes labeled *a-d* in Newman projection VII (Scheme II). Two of these (*c, d*) are orthogonal to the rhenium fragment HOMO (see III) and thus should be less reactive toward electrophiles. Of the remaining two (*a, b*) we had expected that *a*, which is anti to the bulky PPh_3 ligand, would be more reactive toward electrophiles. Schemes II and III clearly show this to be the case. However, the high stereoselectivity observed, $(98 \pm 2):(2 \pm 2)$ or greater, is to us surprising. Hence, the chiral rhenium substituent confers a high degree of reaction asymmetry upon a $\text{C}\equiv\text{C}$ triple bond.

Electrophilic attack upon the acetylide ligand generates a new C_β stereogenic⁴⁰ unit, as shown schematically in Figure 5a. This type of 1,3-asymmetric induction requires an acetylide substituent atom that can increase its valence number past four and is to our knowledge without precedent. There is a conceptual relationship to previously observed stereospecific interconversions of propargyl and allenic systems (Figure 5b).⁴¹ However, here one stereogenic unit is simply converted to another.⁴²

The stereospecific C_α addition of nucleophiles to vinylidene complexes *ac*- and *sc*-**3b** CF_3SO_3^- (Scheme IV) from a direction anti to the PPh_3 ligand has precedent in reactions of the corresponding alkylidene complexes.²² In contrast to the electrophile additions discussed above, there are two stereogenic units in both the reactants and products. Interestingly, Reger has previously reported the stereoselective addition of a methyl cuprate reagent to iron methyl phenyl vinylidene complex $[(\eta^5\text{-C}_5\text{H}_5)\text{Fe}(\text{CO})(\text{PPh}_3)(\text{C}=\text{C}(\text{CH}_3)(\text{C}_6\text{H}_5))]^+\text{CF}_3\text{SO}_3^-$.^{12f} This compound is analogous to **7c** FSO_3^- and hence should exist predominantly as a *sc* $\text{Fe}=\text{C}=\text{C}$ isomer (XII, Scheme III). Transition-state model XIII (Scheme IV) then predicts that the new C_α methyl group should be introduced *cis* to the C_β phenyl group to give an *E* $\text{C}=\text{C}$ isomer. However, Reger reports the predominant (93:7) formation of the less stable *Z* isomer, with the C_α and C_β methyl groups *cis*. This is likely due to the facile interconversion of $\text{Fe}=\text{C}=\text{C}$ isomers (see above), and a less hindered nucleophile C_α approach (*syn* to C_β methyl) in the less stable *ac* isomer. Related phenomena have recently been documented by Brookhart with C_α nucleophilic attack upon the corresponding iron alkylidene complexes.⁴³

(40) Mislow, K.; Siegel, J. *J. Am. Chem. Soc.* **1984**, *106*, 3319.(41) See, inter alia: (a) Cinquini, M.; Colonna, S.; Cozzi, F.; Stirling, C. *J. M. J. Chem. Soc., Perkin Trans. 1* **1976**, 2061. (b) Claesson, A.; Olsson, L.-E. *J. Am. Chem. Soc.* **1979**, *101*, 7302. (c) Corey, E. J.; Boaz, N. W. *Tetrahedron Lett.* **1984**, *25*, 3055.(42) In other relevant work, the "recognition" of stereogenic units separated by a $\text{C}\equiv\text{C}$ triple bond has been probed by NMR: (a) Jones, A. J.; Stiles, P. *J. Tetrahedron Lett.* **1977**, *18*, 1965. Stiles, P. *J. Tetrahedron* **1977**, *33*, 2981. (b) Reisse, J.; Ottinger, R.; Bickart, P.; Mislow, K. *J. Am. Chem. Soc.* **1978**, *100*, 911.(43) Brookhart, M.; Liu, Y.; Buck, R. C. *J. Am. Chem. Soc.* **1988**, *110*, 2337.

Table X. Summary of Rate Constants and Equilibrium and Activation Parameters for Re=C=C Isomerization in Vinylidene Complexes $[(\eta^5\text{-C}_5\text{H}_5)\text{Re}(\text{NO})(\text{PPh}_3)(=\text{C}=\text{CRR}')^+\text{X}^-]$

A. Rate Constants (k_1) for $ac \rightarrow sc$ Re=C=C Isomerization ^a					
compound	temperature (± 0.2 °C)	$k_1 \times 10^4$, s ⁻¹	compound	temperature (± 0.2 °C)	$k_1 \times 10^4$, s ⁻¹
<i>ac</i> -3bCF ₃ SO ₃ ⁻	22.6	1.45 ± 0.08	<i>ac</i> -3dCF ₃ SO ₃ ⁻	17.8	3.00 ± 0.06
	25.2	1.79 ± 0.15		24.6	6.75 ± 0.09
	30.7	3.27 ± 0.13		31.2	14.7 ± 0.45
	36.8	7.62 ± 0.04		41.5	35.7 ± 1.0
<i>ac</i> -3cCF ₃ SO ₃ ⁻	21.9	7.45 ± 0.30	<i>ac</i> -7cFSO ₃ ⁻	27.1	1.28 ± 0.13 ^b
	25.9	9.92 ± 0.02		35.2	2.90 ± 0.20
	34.2	23.8 ± 0.40		39.9	4.36 ± 0.20
	37.1	31.3 ± 1.0		45.0	7.36 ± 0.26

B. Equilibrium and Activation ^c Parameters					
reaction	K_{eq} (21 °C)	ΔG° (21 °C, kcal/mol)	ΔH^\ddagger (kcal/mol)	ΔS^\ddagger (eu)	ΔG^\ddagger (21 °C, kcal/mol)
<i>ac</i> -3bCF ₃ SO ₃ ⁻ ⇌ <i>sc</i> -3bCF ₃ SO ₃ ⁻	1.0 ± 0.1	0.00 ± 0.05	20.8 ± 0.4	-5.7 ± 1.8	22.5 ± 0.9
<i>ac</i> -3cCF ₃ SO ₃ ⁻ ⇌ <i>sc</i> -3cCF ₃ SO ₃ ⁻	4.0 ± 0.4	-0.81 ± 0.07	16.9 ± 0.4	-15.5 ± 1.0	21.5 ± 0.6
<i>ac</i> -3dCF ₃ SO ₃ ⁻ ⇌ <i>sc</i> -3dCF ₃ SO ₃ ⁻	4.0 ± 0.4	-0.81 ± 0.07	18.6 ± 0.3	-10.5 ± 1.5	21.7 ± 0.7
<i>ac</i> -7cFSO ₃ ⁻ ⇌ <i>sc</i> -7cFSO ₃ ⁻	3.0 ± 0.4	-0.64 ± 0.07	17.6 ± 1.3 ^b	-17.7 ± 2.4 ^b	22.8 ± 2.0

^aThe forward rate constant, k_1 , was obtained by plotting $\log([sc]_{\text{equil}} - [sc]_t)$ versus time. The variable k_{-1} was estimated from the slope, $-0.4343(k_1 + k_{-1})$, by substituting k_1/K : Capellos, C.; Bielski, B. H. *J. Kinetic Systems*; Wiley: New York, 1972; Chapter 8. ^bRecalculated from the raw data for ref 25. ^cFor the forward reaction (k_1).

5. Summary. This study establishes that chiral rhenium acetylide and vinylidene complexes $[(\eta^5\text{-C}_5\text{H}_5)\text{Re}(\text{NO})(\text{PPh}_3)(\text{X})]^{n+}$ exhibit a wealth of novel structural and chemical properties. In particular, the 1,3-asymmetric induction observed in C_β electrophilic attack upon acetylide complexes **6b–d** appears without precedent. This study also provides the first quantitative rate and equilibrium data for the interconversion of M=C and M=C=C isomers of corresponding alkylidene and vinylidene complexes. Finally, the scope of the $(\eta^5\text{-C}_5\text{H}_5)\text{Re}(\text{NO})(\text{PPh}_3)$ moiety as a unique stereogenic transmitter has been further extended,⁴⁴ and additional applications of this capability are under active pursuit.

Experimental Section

General Methods. General procedures have been described in a recent paper.²⁴ Additional reagents employed were as follows: (CF₃SO₂)₂O (Aldrich), distilled from P₂O₅, freeze–pump–thaw degassed three times, distilled under vacuum, and stored at -20 °C in an inert atmosphere glovebox; CF₃SO₃H (Aldrich), distilled before use; HPF₆·Et₂O, HBF₄·Et₂O (Columbia), (*n*-C₄H₉)₄N⁺CF₃SO₃⁻ (Alfa), and P(CH₃)₃ (Strem), used as received; TMP (Aldrich),^{27d} distilled from CaH₂. UV/vis spectra were recorded on a Perkin-Elmer 552A spectrophotometer.

Preparation of $(\eta^5\text{-C}_5\text{H}_5)\text{Re}(\text{NO})(\text{PPh}_3)(\text{COCH}_2(1\text{-C}_{10}\text{H}_7))$ (2d**).** A Schlenk flask was charged with $(\eta^5\text{-C}_5\text{H}_5)\text{Re}(\text{NO})(\text{PPh}_3)(\text{CO}_2\text{CH}_3)$ (0.720 g, 1.19 mmol)²⁶ and a stir bar and cooled to -78 °C. Then a -78 °C solution of (1-C₁₀H₇)CH₂MgCl (freshly prepared from (1-C₁₀H₇)C-H₂Cl (1.22 g, 6.94 mmol), toluene (30 mL), and a large excess of magnesium strips) in ether (20 mL) was slowly added via cannula with stirring. The reaction was stirred for 1 h at -78 °C and was then slowly warmed to room temperature. Solvent was removed by rotary evaporation, and the resulting yellow residue was extracted with acetone. The extract was filtered through a medium porosity fritted funnel, and solvent was removed from the filtrate by rotary evaporation. The residue was extracted with a minimum of CH₂Cl₂, and the extract was deposited on a dry 5-cm column of silica gel. The column was eluted with 90:10 (v/v) hexane/ethyl acetate, and the eluent was concentrated by rotary evaporation. A yellow powder precipitated, which was collected by filtration and washed with cold ether (2 × 10 mL) to give **2d** (0.519 g, 0.728 mmol). The washings were concentrated and stored at -20 °C overnight to give a second crop (0.124 g, 0.174 mmol, 76% total yield) of **2d**. The

crops were combined and recrystallized from ether to give golden prisms of **2d** (0.434 g, 0.609 mmol, 51%), mp 195 °C dec: IR (cm⁻¹, thin film) $\nu_{\text{N}=\text{O}}$ 1640 s, $\nu_{\text{C}=\text{O}}$ 1543 s; ¹H NMR (δ , CDCl₃) 7.93–7.00 (m, 3C₆H₅, C₁₀H₇), 5.02 (s, C₅H₅), 4.71 (d, ²J_{HH} = 14.5 Hz, CHH'), 3.52 (d, ²J_{HH} = 14.5 Hz, CHH'); ¹³C{¹H} NMR (ppm, CDCl₃) 249.3 (d, J_{CP} = 9.0 Hz, C=O), PPh₃ at 135.4 (d, J_{CP} = 55.1 Hz, *i*), 133.3 (d, J_{CP} = 10.5 Hz, *o*), 130.1 (s, *p*), 128.2 (d, J_{CP} = 10.7 Hz, *m*), C₁₀H₇ at (s, one resonance obscured) 135.1, 132.4, 127.9, 127.7, 125.8, 125.5, 125.1, 124.9, 124.7, 92.2 (s, C₅H₅), 66.8 (s, CH₂); ³¹P{¹H} NMR (ppm, CDCl₃) 16.2 (s); mass spectrum ((+)-FAB (7 kV, Ar, 3-nitrobenzyl alcohol), *m/z* (rel intensity), ¹⁸⁷Re) 714 (M⁺, 2), 572 (M⁺ - CH₂C₁₀H₇, 100), 544 (M⁺ - COCH₂C₁₀H₇, 25). Anal. Calcd for C₃₃H₂₉NO₂PRE: C, 58.98; H, 4.10. Found: C, 58.76; H, 4.14.

Preparation of $[(\eta^5\text{-C}_5\text{H}_5)\text{Re}(\text{NO})(\text{PPh}_3)(=\text{C}=\text{CH}_2)]^+\text{CF}_3\text{SO}_3^-$ (3aCF₃SO₃**).** A Schlenk flask was charged with $(\eta^5\text{-C}_5\text{H}_5)\text{Re}(\text{NO})(\text{PPh}_3)(\text{COCH}_3)$ (**2a**, 0.600 g, 1.02 mmol; crystalline material recommended),²⁶ CH₂Cl₂ (50 mL), and a stir bar (note: rigorous inert atmosphere techniques are essential throughout this procedure). The solution was cooled to -78 °C, and (CF₃SO₂)₂O (87.0 μL, 0.518 mmol) was added with stirring. After 10 min, TMP^{27d} (172 μL, 1.02 mmol) was added. Stirring was continued for an additional hour at -78 °C, and then (CF₃SO₂)₂O (87.0 μL, 0.518 mmol) was added. After 10 min, the solution was warmed to room temperature and filtered through a medium porosity fritted funnel. Solvent was removed from the filtrate by rotary evaporation, and the resulting orange solid was extracted with CHCl₃. The extract was filtered, and solvent was removed from the filtrate by rotary evaporation. This gave **3aCF₃SO₃** (0.650 g, 0.904 mmol, 88%) as a burnt orange foam, mp 191–194 °C dec: mass spectrum ((+)-FAB (7 kV, Ar, 3-nitrobenzyl alcohol), *m/z* (rel intensity), ¹⁸⁷Re) 570 (M⁺, 100), 544 (M⁺ - C₂H₂, 23), 467 (M⁺ - C₂H₂-C₆H₅, 5), 262 (Ph₃P⁺, 8).

Preparation of $[(\eta^5\text{-C}_5\text{H}_5)\text{Re}(\text{NO})(\text{PPh}_3)(=\text{C}=\text{CHCH}_3)]^+\text{CF}_3\text{SO}_3^-$ (3bCF₃SO₃**).** A Schlenk flask was charged with $(\eta^5\text{-C}_5\text{H}_5)\text{Re}(\text{NO})(\text{PPh}_3)(\text{COCH}_2\text{CH}_3)$ (**2b**, 0.306 g, 0.510 mmol),²⁶ CH₂Cl₂ (80 mL), and a stir bar. The solution was cooled to -78 °C, and (CF₃SO₂)₂O (42.9 μL, 0.255 mmol) was added with stirring. After 10 min, TMP (86.1 μL, 0.510 mmol) was added. The reaction was allowed to warm to 0 °C and then cooled to -78 °C. Then (CF₃SO₂)₂O (42.9 μL, 0.255 mmol) was added. After 10 min, the solution was warmed to room temperature and filtered through a medium porosity fritted funnel. Solvent was removed from the filtrate by rotary evaporation to give crude **3bCF₃SO₃** (0.337 g, 0.460 mmol, 90%) as a light brown powder. The powder was dissolved in CH₂Cl₂, and the resulting solution was layered with ether. Honey yellow needles of **3bCF₃SO₃** formed, which were collected by filtration and dried in vacuo (0.292 g, 0.398 mmol, 78%), mp 152–155 °C dec. This material was a (95 ± 2):(5 ± 2) mixture of *sc/ac* isomers, as assayed by low-temperature ¹H NMR: mass spectrum ((+)-FAB (7 kV, Ar, 3-nitrobenzyl alcohol), *m/z* (rel intensity), ¹⁸⁷Re) 584 (M⁺, 100), 544 (M⁺ - C₂HCH₃, 60), 467 (M⁺ - C₂HCH₃-C₆H₅, 4), 262 (Ph₃P⁺, 6); UV (nm (ε), 3.36 × 10⁻⁵ M in CH₂Cl₂) 256 sh (9100), 267 sh (7500), 272 sh (6000), 280 sh (4100), 312 sh (2200). Anal. Calcd for

(44) See, for example: (a) Crocco, G. L.; Gladysz, J. A. *J. Am. Chem. Soc.* **1985**, *107*, 4103. (b) Heah, P. C.; Patton, A. T.; Gladysz, J. A. *Ibid.* **1986**, *108*, 1185. (c) Fernández, J. M.; Emerson, K.; Larsen, R. D.; Gladysz, J. A. *Ibid.* **1986**, *108*, 8268. (d) Zwick, B. D.; Arif, A. M.; Patton, A. T.; Gladysz, J. A. *Angew. Chem., Int. Ed. Engl.* **1987**, *26*, 910. (e) Fernández, J. M.; Emerson, K.; Larsen, R. D.; Gladysz, J. A. *J. Chem. Soc., Chem. Commun.* **1988**, 37.

$C_{27}H_{24}F_3NO_4PSRe$: C, 44.25; H, 3.27; N, 1.91; P, 4.23. Found: C, 44.72; H, 3.42; N, 1.88; P, 4.27.

Preparation of sc - $[(\eta^5-C_5H_5)Re(NO)(PPh_3)(=C=CHC_6H_5)]^+CF_3SO_3^-$ (sc - $3cCF_3SO_3^-$). This compound was prepared by a procedure identical with that given for $3bCF_3SO_3^-$, utilizing the following materials and quantities: $(\eta^5-C_5H_5)Re(NO)(PPh_3)(COCH_2C_6H_5)$ (**2c**, 0.389 g, 0.588 mmol),²⁶ CH_2Cl_2 (100 mL), $(CF_3SO_2)_2O$ (49.5 μ L, 0.294 mmol), TMP (99.2 μ L, 0.588 mmol), $(CF_3SO_2)_2O$ (49.5 μ L, 0.294 mmol). Crude $3cCF_3SO_3^-$ was obtained as a golden powder (0.390 g, 0.491 mmol, 84%) which was recrystallized from layered CH_2Cl_2 /ether. This gave golden needles of $3cCF_3SO_3^-$ (0.303 g, 0.382 mmol, 65%), mp 205–208 °C dec. This material was a >99:1 mixture of sc/ac isomers, as assayed by low-temperature 1H NMR: mass spectrum ((+)-FAB (7 kV, Ar, 3-nitrobenzyl alcohol), m/z (rel intensity), ^{187}Re) 646 (M^+ , 100), 544 ($M^+ - C_2H_5C_6H_5$, 63). Anal. Calcd for $C_{32}H_{26}F_3NO_4PSRe$: C, 48.35; H, 3.27; N, 1.76; P, 3.90. Found: C, 48.03; H, 3.40; N, 1.75; P, 3.98.

Preparation of sc - $[(\eta^5-C_5H_5)Re(NO)(PPh_3)(=CH(1-C_{10}H_7))]^+CF_3SO_3^-$ (sc - $3dCF_3SO_3^-$). This compound was prepared by a procedure identical with that given for $3bCF_3SO_3^-$, utilizing the following materials and quantities: **2d** (0.179 g, 0.252 mmol), CH_2Cl_2 (50 mL), $(CF_3SO_2)_2O$ (21.5 μ L, 0.128 mmol), TMP (42.5 μ L, 0.252 mmol), $(CF_3SO_2)_2O$ (21.5 μ L, 0.128 mmol). Crude $3dCF_3SO_3^-$ was obtained as a dark yellow residue that was extracted with a minimum of CH_2Cl_2 . Then ether (20 mL) and hexanes (20 mL) were added to the extract. Solvent was removed by rotary evaporation to give $3dCF_3SO_3^-$ as a honey brown powder (0.203 g, 0.240 mmol, 95%), which was crystallized from layered CH_2Cl_2 /hexanes. This gave small yellow prisms of sc - $3dCF_3SO_3^-$ (0.135 g, 0.160 mmol, 63%), mp 218–220 °C dec. This material was a >99:1 mixture of sc/ac isomers, as assayed by low-temperature 1H NMR: mass spectrum ((+)-FAB (7 kV, Ar, 3-nitrobenzyl alcohol), m/z (rel intensity), ^{187}Re) 696 (M^+ , 71), 572 ($M^+ - C_2H_5C_{10}H_7 + CO$, 29), 544 ($M^+ - C_2H_5C_{10}H_7$, 100); UV (nm (ϵ) 2.04×10^5 M in CH_2Cl_2) 260 (33 000), 275 sh (27 000), 300 sh (16 000), 367 (7600). Anal. Calcd for $C_{36}H_{28}F_3NO_4PSRe$: C, 51.18; H, 3.34. Found: C, 50.92; H, 3.40.

Preparation of $(\eta^5-C_5H_5)Re(NO)(PPh_3)(C\equiv CH)$ (6a**).** A Schlenk flask was charged with $3aCF_3SO_3^-$ (0.173 g, 0.241 mmol), CH_2Cl_2 (25 mL), and a stir bar. The solution was cooled to –78 °C, and TMP^{27d} (41.0 μ L, 0.243 mmol) was added with stirring. After 10 min, the mixture was warmed to room temperature and filtered. Solvent was removed from the filtrate by rotary evaporation. The resulting red residue was extracted with THF, and the extract was filtered through a 5-cm plug of silica gel that had been base washed, CH_2Cl_2 washed, and oven-dried. Solvent was removed from the filtrate by rotary evaporation, and the residue was extracted with a minimum of CH_2Cl_2 . Hexanes were added to slightly past a cloud point, and the mixture was filtered through 3 cm of Celite on a medium porosity fritted funnel. The Celite was washed with ether (3 \times 5 mL), and the washings were combined with the filtrate. Solvents were removed by rotary evaporation to give **6a** (0.0726 g, 0.128 mmol, 53%) as an orange powder, mp 211–214 °C dec: mass spectrum (m/z (rel intensity), 17 eV, ^{187}Re) 569 (M^+ , 63), 544 ($M^+ - C_2H_5$, 10), 467 ($M^+ - C_2H_5 - C_6H_5$, 3), 262 (Ph_3P^+ , 100). Anal. Calcd for $C_{25}H_{21}NOPRe$: C, 52.81; H, 3.72. Found: C, 53.12; H, 3.49.

Preparation of $(\eta^5-C_5H_5)Re(NO)(PPh_3)(C\equiv CCH_3)$ (6b**).** A Schlenk flask was charged with $3bCF_3SO_3^-$ (0.200 g, 0.273 mmol), CH_2Cl_2 (50 mL), and a stir bar. The solution was cooled to –78 °C, and TMP (46.0 μ L, 0.273 mmol) was added with stirring. The reaction was allowed to warm to room temperature, and solvent was then removed under oil pump vacuum. This gave crude **6b** as an orange solid (0.140 g, 0.240 mmol, 88%). The solid was dissolved in CH_2Cl_2 , and the solution was layered with hexane. This gave red prisms of **6b**, which were collected by filtration and dried in vacuo (0.130 g, 0.223 mmol, 82%), mp 154–158 °C dec: mass spectrum (m/z (rel intensity), 16 eV, ^{187}Re) 583 (M^+ , 100), 467 ($M^+ - C_2H_5 - C_6H_5$, 13), 262 (Ph_3P^+ , 40). Anal. Calcd for $C_{26}H_{23}NOPRe$: C, 53.59; H, 3.95; N, 2.40; P, 5.32. Found: C, 53.43; H, 3.89; N, 2.37; P, 5.30.

Preparation of $(\eta^5-C_5H_5)Re(NO)(PPh_3)(C\equiv CC_6H_5)$ (6c**).** This compound was prepared by a procedure identical with that given for **6b**, utilizing $3cCF_3SO_3^-$ (0.200 g, 0.252 mmol) and TMP (42.0 μ L, 0.250 mmol). Crude **6c** was obtained as an orange powder (0.150 g, 0.233 mmol, 92%), which was recrystallized from layered CH_2Cl_2 /ether. This gave orange needles of **6c**, which were collected by filtration and dried in vacuo (0.121 g, 0.188 mmol, 75%), mp 205–208 °C: mass spectrum (m/z (rel intensity), 16 eV, ^{187}Re) 645 (M^+ , 92), 544 ($M^+ - C_2C_6H_5$, 15), 467 ($M^+ - C_2C_6H_5 - C_6H_5$, 10), 262 (Ph_3P^+ , 100). Anal. Calcd for $C_{31}H_{25}NOPRe$: C, 57.74; H, 3.88; N, 2.17; P, 4.81. Found: C, 57.08; H, 4.06; N, 2.24; P, 4.61.

Preparation of $(\mu^5-C_5H_5)Re(NO)(PPh_3)(C\equiv C(1-C_{10}H_7))$ (6d**).** A Schlenk flask was charged with $3dCF_3SO_3^-$ (0.245 g, 0.290 mmol), CH_2Cl_2 (30 mL), and a stir bar. The solution was cooled to –78 °C, and TMP (49.0 μ L, 2.90 mmol) was added with stirring. After 5 min, the

mixture was warmed to room temperature and then filtered through a medium porosity fritted funnel. Solvent was removed from the filtrate by rotary evaporation. The resulting red powder was extracted with CH_2Cl_2 , and the extract was filtered through a 5-cm plug of silica gel that had been washed with 90:10 (v/v) hexanes/ NEt_3 , CH_2Cl_2 , and dried. Hexanes were added to the filtrate, and solvent was removed by rotary evaporation. This gave **6d** as an orange foam (0.167 g, 0.241 mmol, 83%). The foam was dissolved in CH_2Cl_2 , and the solution was layered with hexane. This gave orange needles of **6d** that were collected by filtration and dried in vacuo (0.144 g, 0.208 mmol, 72%), mp 209 °C dec: mass spectrum (m/z (rel intensity), 17 eV, ^{187}Re) 695 (M^+ , 100%), 262 (Ph_3P^+ , 13); UV (nm (ϵ), 2.58×10^5 M in CH_2Cl_2) 260 (23 000), 284 sh (16 000), 320 (16 000), 360 sh (7900) 398 sh (2300). Anal. Calcd for $C_{35}H_{27}NOPRe$: C, 60.50; H, 3.92. Found: C, 60.23; H, 4.03.

Reactions of Acetylide Complexes with CF_3SO_3H . In a typical experiment, a 5-mm NMR tube was charged with **6b-d** (0.0465 mmol) and CD_2Cl_2 (0.600 mL) and capped with a septum. The solution was freeze-pump-thaw degassed three times, and a nitrogen atmosphere was admitted. The tube was cooled to –196 °C, and CF_3SO_3H (4.50 μ L, 0.0508 mmol) was added via syringe. The mixture was thawed in a –78 °C bath, shaken, and quickly transferred to a –80 °C NMR probe. Immediate analysis by 1H NMR gave the ac/sc ratios given in the Results section.

Preparation of sc - $3dPF_6^-$. A Schlenk flask was charged with **6d** (0.0147 g, 0.0212 mmol), CH_2Cl_2 (15 mL), and a stir bar. The solution was cooled to –78 °C, and then $HPF_6 \cdot Et_3O$ (0.0047 g, 0.021 mmol) was added with stirring. After 5 min, the mixture was warmed to room temperature, and solvent was removed under oil pump vacuum. The resulting yellow residue was extracted with CH_2Cl_2 , and the extract was layered with hexanes. This gave yellow prisms of sc - $3dPF_6^-$, which were collected by filtration and dried in vacuo (0.0119 g, 0.0142 mmol, 67%), mp 224 °C dec. The IR and NMR (1H , ^{13}C , ^{31}P) spectra, and low-temperature isomer purity assay, of sc - $3dPF_6^-$ matched those of sc - $3dCF_3SO_3^-$. Anal. Calcd for $C_{35}H_{28}F_6NOP_2Re$: C, 50.00; H, 3.36. Found: C, 49.61; H, 3.49.

Preparation of $[(\eta^5-C_5H_5)Re(NO)(PPh_3)(=C=C(CH_3)_2)]^+FSO_3^-$ (7b FSO₃⁻**).** A Schlenk flask was charged with **6b** (0.200 g, 0.343 mmol), CH_2Cl_2 (50 mL), and a stir bar. The solution was cooled to 0 °C, and CH_3SO_3F (47.0 μ L, 0.547 mmol) was added with stirring. The mixture was allowed to warm to room temperature over the course of 45 min, then solvent was removed under reduced pressure, and the residue was washed with toluene until the washings were colorless. The remaining golden solid was dissolved in CH_2Cl_2 (20 mL), and the solution was layered with ether. Light brown needles of **7b FSO₃⁻** formed over the course of 2 days and were collected by filtration and dried in vacuo (0.190 g, 0.273 mmol, 80%). Anal. Calcd for $C_{27}H_{26}FNO_4PSRe$: C, 46.54; H, 3.73; N, 2.01; P, 4.45. Found: C, 45.86; H, 3.82; N, 1.98; P, 4.40.

Preparation of $[(\eta^5-C_5H_5)Re(NO)(PPh_3)(=C=C(CH_3)(C_6H_5))]^+FSO_3^-$ (7c FSO₃⁻**).** This compound was prepared by a procedure identical with that given for **7b FSO₃⁻**, utilizing **6c** (0.250 g, 0.388 mmol), CH_3SO_3F (50.0 μ L, 0.582 mmol), and CH_2Cl_2 (50 mL). The solid remaining after the toluene wash was recrystallized from layered CH_2Cl_2 /ether. Brown needles of **7c FSO₃⁻** formed, which were collected by filtration and dried in vacuo (0.200 g, 0.264 mmol, 68%): IR (cm^{-1} , $CHCl_3$) $\nu_{N=O}$ 1750 s, $\nu_{C\equiv C}$ 1652 m; 1H NMR spectrum (room temperature) indicated an ca. 75:25 sc -**7c FSO₃⁻**/ ac -**7c FSO₃⁻** ratio (δ , $CDCl_3$) ac 7.78–7.08 (m, $3C_6H_5$), 7.08–6.10 (m, $1C_6H_5$), 6.09 (s, C_5H_5), 2.33 (s, CH_3), sc 7.78–7.08 (m, $4C_6H_5$), 6.06 (s, C_5H_5), 1.58 (s, CH_3); $^{13}C\{^1H\}$ NMR (ppm, $CDCl_3$) ac 334.2 (d, $J_{CP} = 10.0$ Hz, C_a), 141.2 (s, C_β), 132.9–128.1 (PC_6H_5 and CC_6H_5), 98.5 (s, C_5H_5), 16.8 (s, CH_3), sc 330.9 (weak m, C_a), 140.0 (s, C_β), 133.1–125.9 (m, PC_6H_5 and CC_6H_5), 98.9 (s, C_5H_5), 10.6 (s, CH_3); mass spectrum ((+)-FAB (7 kV, Ar, 3-nitrobenzyl alcohol), m/z (rel intensity), ^{187}Re) 660 (M^+ , 100), 544 ($M^+ - C_2(CH_3)C_6H_5$, 33), 467 ($544 - C_6H_5$, 7), 262 (Ph_3P^+ , 5).

Preparation of $[(\eta^5-C_5H_5)Re(NO)(PPh_3)(C(P(CH_3)_3)=C(CH_3)_2)]^+CF_3SO_3^-$ (8CF₃SO₃⁻**).** A Schlenk flask was charged with **6b** (0.0404 g, 0.0693 mmol), CH_2Cl_2 (20 mL), and a stir bar. The solution was cooled to 0 °C, and $CF_3SO_3CH_3$ (9.40 μ L, 0.829 mmol) was added with stirring. The mixture was warmed to room temperature over 45 min, and solvents were removed by rotary evaporation. The resulting brown residue was washed with toluene until the washings were colorless. The residue was then extracted with CH_2Cl_2 (20 mL). A 50-mL Schlenk flask was charged with this extract and a stir bar. The mixture was cooled to 0 °C, and $P(CH_3)_3$ (10.0 μ L, 0.0983 mmol) was added with stirring. After 45 min, solvents were removed under oil pump vacuum. This gave an orange residue that was extracted with CH_2Cl_2 . The extract was layered with ether. This gave orange needles of **8CF₃SO₃⁻**, which were collected by filtration and dried in vacuo (0.0345 g, 0.0419 mmol, 60%), mp 211 °C: IR (cm^{-1} , thin film) $\nu_{N=O}$ 1649 s; 1H NMR (δ , $CDCl_3$) 7.50–7.25 (m, $3C_6H_5$), 5.44 (s, C_5H_5), 2.14 (d, $J_{HP} = 2.5$ Hz, $E-CH_3$), 1.75 (d, $J_{HP} = 12.2$ Hz, $3PCH_3$), 1.43 (d, $J_{HP} = 1.7$ Hz, $Z-CH_3$); $^{13}C\{^1H\}$ NMR

(ppm, CDCl₃) 161.5 (d, J_{CP} = 6.1 Hz, C_β), 103.4 (dd, $^1J_{CP}$ = 16.6 Hz, $^2J_{CP}$ = 7.6 Hz, C_α), PPh₃ at 134.4 (d, J_{CP} = 52.1 Hz, *i*), 133.1 (d, J_{CP} = 8.6 Hz, *o*), 130.4 (s, *p*), 128.3 (d, J_{CP} = 8.5 Hz, *m*), 120.4 (q, J_{CF} = 319.4 Hz, CF₃), 92.1 (s, C₅H₅), 37.4 (dd, $^3J_{CP}$ = 27.1 Hz, $^4J_{CP}$ = 2.8 Hz, Z-CH₃), 27.1 (d, J_{CP} = 16.1 Hz, E-CH₃), 16.6 (d, J_{CP} = 53.1 Hz, PCH₃); $^{31}\text{P}\{^1\text{H}\}$ NMR (ppm, CDCl₃) 23.0 (s, PCH₃), 7.5 (s, PPh); mass spectrum ((+)-FAB (7 kV, Ar, 3-nitrobenzyl alcohol), *m/z* (rel intensity), ^{187}Re) 674 (M⁺, 37), 598 (M⁺ - P(CH₃)₃, 100), 544 (M⁺ - C(P(CH₃)₃)C(CH₃)₂, 23), 412 (M⁺ - PPh₃, 37). Anal. Calcd for C₃₁H₃₅F₃NO₄P₂SRe: C, 45.25; H, 4.29. Found: C, 45.11; H, 4.31.

Preparation of (Z)-[(η⁵-C₅H₅)Re(NO)(PPh₃)(C(P(CH₃)₃)=CHCH₃)]⁺CF₃SO₃⁻ ((Z)-9CF₃SO₃⁻). Complex *ac*-3bCF₃SO₃⁻ was prepared in a septum-capped NMR tube at -78 °C as described above utilizing **6b (0.0250 g, 0.0429 mmol), CF₃SO₃H (3.80 μL, 0.0429 mmol), and CD₂Cl₂ (0.600 mL). Then P(CH₃)₃ (55.0 μL, 0.540 mmol) was added, and the sample was quickly transferred to a -80 °C NMR probe (data: text). The sample was kept at room temperature for a day and was then transferred to a flask where solvent was removed by oil pump vacuum. The resulting red residue was extracted with CH₂Cl₂. The extract was layered with ether. This gave red flowers of (Z)-9CF₃SO₃⁻, which were collected by filtration and dried in vacuo (0.0198 g, 0.0245 mmol, 57%) dec point 222 °C: IR (cm⁻¹, thin film) $\nu_{\text{N=O}}$ 1649 s; ^1H NMR (δ, CDCl₃) 7.50–7.26 (m, 3C₆H₅), 6.93 (dq, $^3J_{HP}$ = 36.3 Hz, $^3J_{HH}$ = 6.4 Hz, =CH), 5.48 (s, C₅H₅), 1.49 (d, J_{HP} = 12.5 Hz, 3PCH₃), 1.40 (dd, $^3J_{HH}$ = 6.3 Hz, $^4J_{HP}$ = 3.0 Hz, CCH₃); $^{13}\text{C}\{^1\text{H}\}$ NMR (ppm, CDCl₃) 151.4 (d, J_{CP} = 3.8 Hz, C_β), 115.1 (dd, $^1J_{CP}$ = 22.2 Hz, $^2J_{CP}$ = 8.0 Hz, C_α), PPh₃ at 135.1 (d, J_{CP} = 52.6 Hz, *i*), 133.2 (d, J_{CP} = 10.1 Hz, *o*), 130.6 (s, *p*), 128.4 (d, J_{CP} = 10.1 Hz, *m*), 92.0 (s, C₅H₅), 24.4 (d, J_{CP} = 29.7 Hz, CCH₃), 12.2 (d, J_{CP} = 55.5 Hz, PCH₃); $^{31}\text{P}\{^1\text{H}\}$ NMR (ppm, CDCl₃) 30.5 (s, PCH₃), 5.8 (s, PPh); mass spectrum ((+)-FAB (7 kV, Ar, 3-nitrobenzyl alcohol), *m/z* (rel intensity), ^{187}Re) 660 (M⁺, 100), 584 (M⁺ - P(CH₃)₃, 99), 544 (M⁺ - C(P(CH₃)₃)CHCH₃, 53), 467 (544 - C₆H₅, 11), 398 (M⁺ - PPh₃, 30). Anal. Calcd for C₃₀H₃₃F₃NO₄P₂SRe: C, 44.55; H, 4.11. Found: C, 44.38; H, 4.15.**

Preparation of (E)-[(η⁵-C₅H₅)Re(NO)(PPh₃)(C(P(CH₃)₃)=CHCH₃)]⁺CF₃SO₃⁻ ((E)-9CF₃SO₃⁻). A 5-mm septum-capped NMR tube was charged with crystalline **3bCF₃SO₃⁻ (0.0314 g, 0.0429 mmol, (95 ± 2):(5 ± 2) *sc/ac* mixture) and cooled to -78 °C. Then CD₂Cl₂ (0.600 mL, -78 °C) was added. The tube was shaken, P(CH₃)₃ (55.0 μL, 0.540 mmol) was added, and the mixture was quickly transferred to an -80 °C NMR probe (data: text). The sample was kept at room temperature for a day and was then transferred to a flask where solvent was removed by oil pump vacuum. The resulting red residue was extracted with ether and filtered. An equal volume of hexanes were added, and the solution was again filtered. Solvent was removed from the filtrate by rotary evaporation to give (E)-9CF₃SO₃⁻ as an orange powder, which was dried in vacuo (0.0278 g, 0.0344 mmol, 80%), mp 185 °C: IR (cm⁻¹, thin film) $\nu_{\text{N=O}}$ 1649 s; ^1H NMR (δ, CDCl₃) 7.48–7.27 (m, 3C₆H₅), 6.13 (dq, $^3J_{HP}$ = 60.7 Hz, $^3J_{HH}$ = 7.3 Hz, =CH), 5.27 (s, C₅H₅), 1.89 (d, J_{HP} = 12.6 Hz, 3PCH₃), 1.75 (dd, $^3J_{HH}$ = 7.3 Hz, $^4J_{HP}$ = 3.3 Hz, CCH₃); $^{13}\text{C}\{^1\text{H}\}$ NMR (ppm, CDCl₃) 159.8 (dd, $^1J_{CP}$ = 6.8 Hz, $^2J_{CP}$ = 3.8 Hz, C_β), 108.3 (dd, $^1J_{CP}$ = 16.7 Hz, $^2J_{CP}$ = 7.5 Hz, C_α), PPh₃ at 133.6 (d, J_{CP} = 53.3 Hz, *i*), 133.6 (d, J_{CP} = 10.1 Hz, *o*), 130.9 (s, *p*), 128.7 (d, J_{CP} = 10.3 Hz, *m*), 120.6 (q, J_{CF} = 320.2 Hz, CF₃), 91.0 (s, C₅H₅), 22.7 (d, J_{CP} = 16.4 Hz, CCH₃), 14.9 (d, J_{CP} = 53.4 Hz, PCH₃); $^{31}\text{P}\{^1\text{H}\}$ NMR (ppm, CDCl₃) 26.5 (s, PCH₃), 17.7 (s, PPh); mass spectrum ((+)-FAB (7 kV, Ar, 3-nitrobenzyl alcohol), *m/z* (rel intensity), ^{187}Re) 660 (M⁺, 49), 584 (M⁺ - P(CH₃)₃, 100), 544 (M⁺ - C(P(CH₃)₃)CHCH₃, 60), 467 (544 - C₆H₅, 22), 398 (M⁺ - PPh₃, 30).**

Photolysis Experiments. In a typical experiment, a septum-capped NMR tube was charged with **3c**CF₃SO₃⁻ or **3d**CF₃SO₃⁻ (0.0400 mmol) and CD₂Cl₂ (0.600 mL). The resulting solution was freeze-pump-thaw degassed three times, and an N₂ atmosphere was admitted. The tube was placed in a large Pyrex test tube that are partially filled with acetone. The test tube was in turn placed in a large unsilvered Pyrex Dewar charged with a dry ice/acetone bath. A Hanovia 450-W lamp was suspended in a water-cooled quartz immersion well placed adjacent to the Dewar. The sample was irradiated for 3 h at -78 °C and then quickly transferred to an -80 °C NMR probe. Analysis by ^1H NMR indicated a (50 ± 2):(50 ± 2) photostationary state of *sc/ac* Re=C=C isomers. The sample was allowed to return to thermodynamic equilibrium (dark, room temperature), and additional irradiation cycles were conducted without noticeable decomposition.

Rate Experiments. A septum-capped NMR tube was charged with **6b-d** (0.0300 mmol) and CD₂Cl₂. The resulting solution was freeze-pump-thaw degassed three times, and an N₂ atmosphere was admitted. Then *ac*-**3b-d**CF₃SO₃⁻ were generated as above, and the tube was quickly transferred to an NMR probe that had been preequilibrated to the appropriate temperature. The disappearance of *ac*-**3b-d**CF₃SO₃⁻ and appearance of *sc*-**3b-d**CF₃SO₃⁻ were monitored by integration of the following ^1H NMR resonances: *ac*-**3b**CF₃SO₃⁻ and *sc*-**3b**CF₃SO₃⁻, CH₃; *sc*-**3c-d**CF₃SO₃⁻, =C=CH; *ac*-**3c-d**CF₃SO₃⁻, the upfield aromatic proton. Calculation of k_1 : see Table X. All ΔH^\ddagger and ΔS^\ddagger were calculated from $\ln(k_1/T)$ versus $1/T$ plots. Other rate experiments were conducted similarly.

X-ray Crystal Structure of *sc*-3dPF₆⁻. A large yellow crystal of *sc*-**3d**PF₆⁻ (see above) was cleaved to give a fragment suitable for X-ray crystallography. The fragment was mounted on a glass fiber with epoxy cement and then coated with epoxy cement. Data were collected as summarized in Table 11. Lattice parameters were determined for 15 centered reflections with 2θ between 16° and 24°.

The unit cell was monoclinic, and the pattern of systematic absence was consistent with either centric space group *C2/c* (no. 15) or acentric space group *Cc* (no. 9). Statistics indicated a centric structure, so space group *C2/c* was used in subsequent analysis.

The structure was solved by standard heavy atom techniques with the UCLA crystallographic package of programs.⁴⁵ The position of the rhenium was computed from a Patterson map. After a cycle of least-squares refinement, an electron density difference map was computed. This gave the positions of all non-hydrogen atoms. Absorption corrections (ψ scan technique; ψ scan reflections 111, 333, 555, max/min intensity 1.29) were applied. After several cycles of refinement, the hydrogen atom positions were computed (C-H distance 1.0 Å), and isotropic thermal parameters were assigned to the individual hydrogens that were approximately equal to the isotropic thermal parameter of the carbon to which they were bond. All non-hydrogen atoms were then refined with anisotropic thermal parameters.

X-ray Crystal Structure of **6b.** X-ray data were collected on red prisms of **6b** (see above) as summarized in Table 11, employing techniques that have been previously described.⁴⁶ Lattice parameters (Table 1) were determined analogously to the previous structure. The position of the rhenium was located from a three-dimensional Patterson map. Full-matrix least-squares refinement yielded all non-hydrogen atoms.⁴⁵ Absorption corrections were applied, and all non-hydrogen atoms were refined with anisotropic temperature factors, except for C(14), which had a negative temperature factor when refined anisotropically. Phenyl and methyl hydrogens were located from a difference Fourier map. The cyclopentadienyl hydrogen positions were computed as above.

Acknowledgment. We thank the Department of Energy and NIH for support of this research.

Registry No. **2a**, 82582-46-5; **2b**, 82582-47-6; **2c**, 82582-48-7; **2d**, 115365-02-1; **3a** CF₃SO₃⁻, 82582-34-1; *sc*-**3b** CF₃SO₃⁻, 82637-17-0; *ac*-**3b** CF₃SO₃⁻, 82582-36-3; *sc*-**3c** CF₃SO₃⁻, 82659-75-4; *ac*-**3c** CF₃SO₃⁻, 82582-38-5; *sc*-**3d** CF₃SO₃⁻, 115365-04-3; *sc*-**3d** PF₆⁻, 115405-78-2; *ac*-**3d** CF₃SO₃⁻, 115405-77-1; **6a**, 82582-43-2; **6b**, 82582-44-3; **6c**, 82582-45-4; **6d**, 115365-05-4; **7b** FSO₃⁻, 82598-62-7; *sc*-**7c** FSO₃⁻, 82637-19-2; *ac*-**7c** FSO₃⁻, 82582-42-1; **8** CF₃SO₃⁻, 115365-07-6; (Z)-**9** CF₃SO₃⁻, 115365-09-8; (E)-**9** CF₃SO₃⁻, 115405-80-6; (η⁵-C₅H₅)Re(NO)(PPh₃)(CO₂CH₃), 82293-79-6; (1-C₁₀H₇)CH₂MgCl, 37846-72-3.

Supplementary Material Available: Tables of hydrogen atom coordinates and isotropic and anisotropic temperature factors for **3d**PF₆⁻ and **6b** (4 pages); tables of observed and calculated structure factors (36 pages). Ordering information is given on any current masthead page.

(45) Programs employed included CARESS (R. W. Broach, Argonne National Laboratory; CARESS incorporated features of PROFILE: Blessing, R. G.; Coppend, P.; Becker, P. J. *Appl. Cryst.* **1972**, *7*, 488), NORMAL, EXFFT, and SEARCH (all from the MULTAN 80 package, Peter Main, Department of Physics, University of York, York, England), ORFLS (ORNL-TM-30-5), ORFFE (ORNL-TM-306), and ORTEP (ORNL-TM-5138).

(46) Strouse, J.; Layten, S. W.; Strouse, C. E. *J. Am. Chem. Soc.* **1977**, *99*, 562.